JSC INTERNAL NOTE NO. 77-FM-19

April 12, 1977

APPLICATION AND ANALYSIS OF SATELLITE ORBIT PREDICTION TECHNIQUES

Software Development Branch

MISSION PLANNING AND ANALYSIS DIVISION

National Aeronautics and Space Administration

LYNDON B. JOHNSON SPACE CENTER

Houston, Texas

JSC-12571

JSC INTERNAL NOTE NO. 77-FM-19

SHUTTLE PROGRAM

APPLICATION AND ANALYSIS OF SATELLITE ORBIT PREDICTION TECHNIQUES

By Analytical and Computational Mathematics, Inc.

April 12, 1977

MISSION PLANNING AND ANALYSIS DIVISION
NATIONAL AERONAUTICS AND SPACE ADMINISTRATION
JOHNSON SPACE CENTER
HOUSTON, TEXAS

JSC Task Monitor: George A. Weisskopf

Approved: Elric N McHenry
Elric N. McHenry, Chief
Software Development Branch

Approved:
Ronald L. Berry, Chief
Mission Planning and Analysis Division

PREFACE

Mathematical methods for computing satellite orbits consist of an algorithm of formulas that can be programed on an automatic computer. This report is concerned, specifically, with methods for predicting satellite orbits; that is, given the satellite's state vector (usually position and velocity) at an epoch, compute the state vector at another epoch (or sequence of epochs). A large variety of methods and techniques are available today for solving this problem and it is necessary to choose one that best suits a particular application. To do this, the methods must be converted into an executable program code and then analyzed to determine their efficiency and accuracy for producing usable results.

Each method consists of three basic parts:

a. Formulation of the differential equations of motion,

b. Analytical or numerical method for the solution (integration) of these equations,

c. Mathematical model of the perturbing forces acting on the satellite.

Each part can be coded as a separate module or subroutine in a computer program. The formulations (part a) are discussed in section 1.0 of this report. New formulations are available that have a profound impact on increasing the efficiency of orbit predictions. This is due to the new stabilized differential equations that are easier to solve. The methods of integration (part b) are also discussed in section 1.0. The aim is to match formulation and integration method for a particular application. Mathematical force models (part c) are discussed in section 2.0.

In section 1.0 of this report, the concern is with "numerical accuracy" in the orbit prediction. This is defined to mean the accuracy to which the differential equations are solved, assuming that the programed equations perfectly describe the physical situation. The most recent advances in celestial mechanics and numerical analysis are examined. A set of rigorous numerical experiments were carried out to test the various combinations of formulation and integrator.

The subject of force models is concerned with "physical accuracy" of an orbit predictor. That is, how well does the predicted orbit agree to physical reality? This depends, usually, on how well the forces can be modeled. Several types of perturbing forces that affect the orbit are discussed in section 2.0. Questions to be considered are:

- What are the typical magnitudes of each perturbation? If they are neglected or poorly modeled, how is the accuracy of an orbit prediction affected?

- How can the force routines be made less costly in terms of computer runtime and storage? What new, more efficient force models should be used?

- What are the necessary force models for a variety of standard Earth satellite orbits?

The suggestions and recommendations contained in this report are based on the particular cases studied. An attempt was made to consider a variety of orbits, prediction intervals, output requirements, etc. In view of the wide variety of satellite missions that are being planned, the scope of this study is necessarily limited. Nevertheless, it is hoped that these results and conclusions will be a useful guide in choosing the components of an orbit prediction program, as well as a help in analyzing the numerical results of such a program.

CONTENTS

TABLES

FIGURES

APPLICATION AND ANALYSIS OF SATELLITE ORBIT PREDICTION TECHNIQUES

By Analytical and Computational Mathematics, Inc.

1.0 FORMULATIONS AND INTEGRATION METHODS

1.1 Introduction

The computation and prediction of satellite orbits requires the solution of a set of ordinary differential equations. Studies have been carried out to determine the best methods for obtaining these solutions. It will be assumed in this section that the perturbing forces are known exactly. The goal, therefore, is to investigate the numerical accuracy of a satellite orbit computation program. That is, to determine the effects of roundoff and truncation errors on the solution.

Many different formulations of the satellite differential equations are available. Of special interest here are the new formulations that have the mean motion based on the total energy. They will be compared to the more classical formulations and evaluated via numerical experiments.

Methods for the numerical solution of ordinary differential equations are also discussed. Numerical experiments have been carried out to determine the most efficient methods, in terms of computer cpu times.

An intention of these studies has been to determine the formulation and numerical integration combinations which exhibit most or all of the following attributes.

a. Numerically Accurate: The combination should produce solutions which are consistently more accurate than the force model accuracy (see section 2.0 on force model errors). In other words, roundoff and truncation errors should be much smaller than modeling errors.

b. Predictable Accuracy: In addition to point (a), the accuracy of the solution should be predictable. In practical applications, it is necessary that an upper bound on the error be known.

c. Efficient: For a given accuracy, a combination should require as little computation time as possible to obtain the

solution. Thus it is desirable to have a method which is reasonably accurate but requires the least computation time.

d. Reliable: A combination should give reliable results for all possible applications. In addition, the combination should have a "built-in" reliability so that it is insensitive to possible misuse of the algorithm.

e. Stable: Small errors in the initial state should not cause the combination to run into numerical difficulties. Some combinations may be reliable over short propagation times; but, because of instabilities become completely erroneous for longer times.

f. General: The formulation should be valid over the whole range of intitial conditions. For instance, certain sets have singularities for circular or equatorial orbits. However, since we are most interested in elliptical orbits, we will exclude the generality to parabolic or hyperbolic orbits.

g. Concise: The computer algorithm for a combination should require a small percentage of the storage requirements of the total force model.

A brief discussion is given on analytical and seminumerical methods. These are specialized techniques that allow a large savings in computer time. Their accuracy and range of applications will be discussed.

1.2 Formulations

The satellite differential equations can be formulated in a number of different ways for different purposes. All formulations fall basically into three classes:

a. Coordinate Formulation

b. Variation of Parameters

c. Total Energy Elements

These three classes can each be divided into two sets, formulations with time as the independent variable and formulations with an independent variable other than time. Before discussing the different classes one should understand the effect of the independent variable on the numerical integration. The ellipses of figure 1 show where the force model is being evaluated for equal steps in three different independent variables. The perigee point of this ellipse (e = .7) is located on the right-hand side. Note that equal steps in the true anomaly tends to evaluate the force model more near the perigee point. On the other hand, equal steps in time tends to bunch the majority of the force

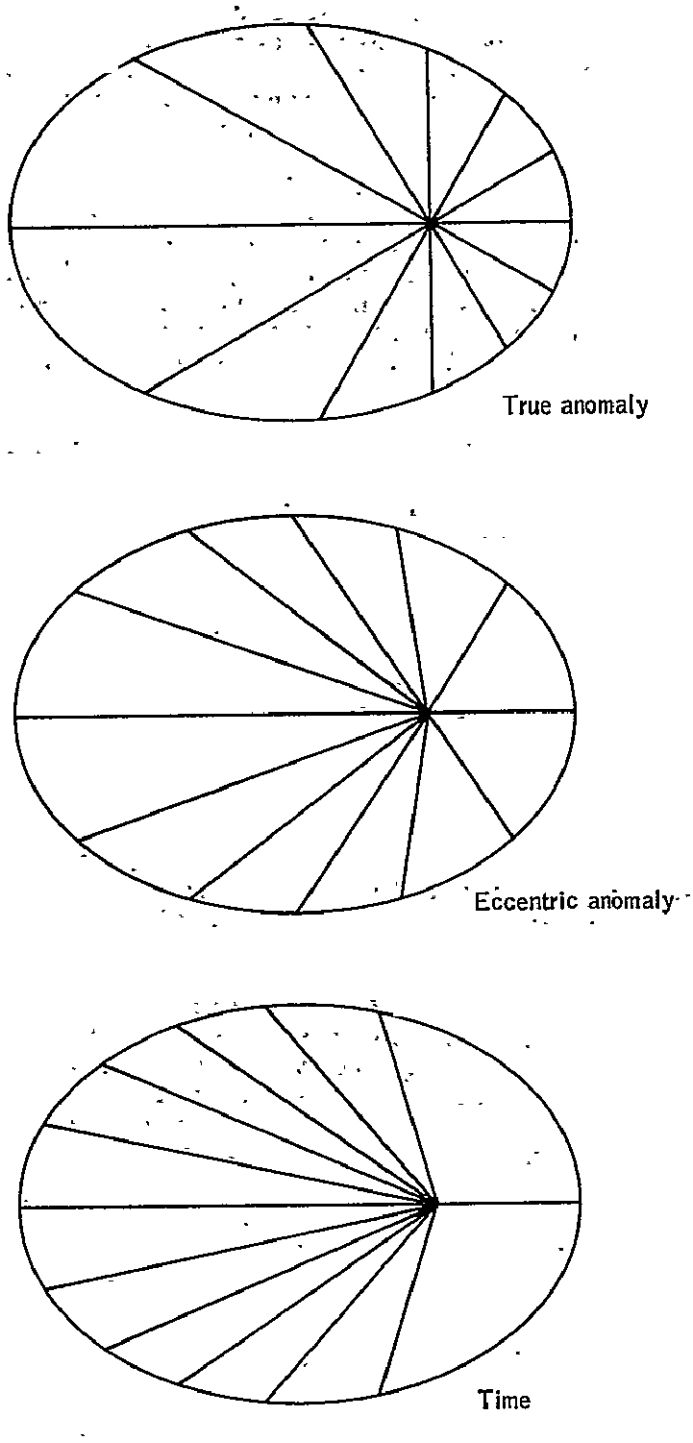

Figure 1.- Independent variables.

evaluations near the apogee. The eccentric anomaly smooths the evaluations equally over perigee and apogee. Since the stronger perturbations are usually associated with the perigee point (atmospheric drag, for example), it becomes immediately clear why the use of the true or eccentric anomaly results in an automatic "analytical" step size control.

One could conclude from figure 1 that if the perturbations are much stronger at perigee than at apogee, then the true anomaly would be the most appropriate choice for independent variable. If the perturbations at apogee and perigee were nearly equal then one might expect the eccentric anomaly to be the better choice. Clearly, time would be a poor choice for either case. Of course, when the orbit is circular then the different independent variables become quite the same.

1.2.1 Coordinate formulation.- Let the coordinates $\vec{x}$ of the satellite be referred to an inertial rectangular coordinate system. The most basic formulation of the equations of motion is the so called Cowel method (ref. 1)

$$\ddot{\vec{x}} = -\frac{\mu \vec{x}}{r^3} - \frac{\partial V}{\partial \vec{x}} + \vec{P}$$

where

$$r = |\vec{x}|$$

V is the perturbing potential function and $\vec{P}$ represents accelerations that are not derivable from a potential. The gravitational parameter is μ. This method uses time as the independent variable. The main advantage is, of course, it's simplicity. The approach, however, has several disadvantages. The right-hand side of the differental equations are quite large and therefore one is forced to take small numerical steps or use a high order integrator. Also, the differential equations are unstable. An attempt to alleviate the first problem was made by Encke (ref. 1). If the equation of unperturbed motion is

$$\ddot{\vec{\zeta}} + \mu \frac{\vec{\zeta}}{\zeta^3} = 0$$

and

$$\Delta\vec{x} = \vec{x} - \vec{\zeta}$$

Then the Encke equations read

$$\ddot{\Delta\vec{x}} = \vec{F} + \mu\left(\frac{\vec{\zeta}}{|\vec{\zeta}|^3} - \frac{\vec{x}}{r^3}\right)$$

where

$$\vec{F} = -\frac{\partial V}{\partial \vec{x}} + \vec{P}$$

The right-hand side of the equation is small if $\Delta\vec{x}$ is small. But $\Delta\vec{x}$ may grow to be quite large, therefore, this method must be "rectified." This rectification involves setting $\vec{\xi} = \vec{x}$ and $\Delta\vec{x} = 0$. This can cause additional instabilities in the differential equations.

One may modify the Cowell equations by using a fictitious time s, defined by the differential equation

$$\frac{dt}{ds} = t' = r$$

The equations of motion then become

$$\vec{x}'' = \frac{r'}{r}\vec{x}' - \frac{\mu}{r}\vec{x} + r^2\vec{F}$$

This method (ref. 2) retains the coordinate formulation and adds an important analytic stepsize control, but it requires an extra differential equation to compute the time. An Encke-type formulation can also be applied to these equations to reduce the magnitude of the right hand side of the differential equations.

1.2.2 Variation of parameters.- By solving the unperturbed problem one obtains a vector of six constants of integration $\vec{\alpha}$. Classical variation of parameters (VOP) methods develop equations of motion which define how the six constants of integration vary in the perturbed case. They have the form

$$\dot{\vec{\alpha}} = \vec{f}(\vec{\alpha}, t, \vec{F})$$

The right-hand sides of the differential equations are small, as in the Encke method, but do not require the expense of rectification.

The Lagrange and Deluanay element formulations are typical VOP examples. These sets, however, have singularities at zero inclination and zero eccentricity. Another example, the Poincare' elements, avoids these problems. These VOP elements, which prove very fruitful in analytical studies, are somewhat cumbersome for numerical integration. Since the forces are usually given in Cartesian coordinates, the differential equations require a conversion from $\vec{\alpha}$ and t to $\vec{x}$. Another method, developed by Pines (ref. 3), simplifies this conversion. This method, developed with time as the independent variable, has mixed secular terms. These terms grow in magnitude with time and will eventually degrade the accuracy of the solution. The secular terms were later eliminated by a conversion to a perturbed time as independent variable (ref. 4). Another disadvantage of these classical variation of parameter methods is that a costly iteration to solve Kepler's equation is required at each integration step (ref. 5).

Burdet has developed a VOP method based on Sperling's solution of a set of regular and linear differential equations of the unperturbed (two-body) motion (ref. 6). Although this approach requires 14 differential equations, it provides increased numerical stability. The method presents no mixed secular terms and requires no Kepler iteration. The regularization requires a transformation to an independent variable other than time. For elliptical cases the method can be specialized so that the independent variable becomes the eccentric anomaly and thus this method also has an analytical step size control (ref. 7).

1.2.3 Total energy elements.- Kustaanheimo and Stiefel have also developed a linear and regular set of differential equations. The resultant differential equation is that of a perturbed harmonic oscillator in 4-space

$$\vec{u}'' + \omega\vec{u} = Q\left(V, \frac{\partial V}{\partial \vec{x}}, \vec{P}\right)$$

where

$$\frac{dt}{ds} = t' = r$$

However, the major difference between the Burdet and KS method is that the total energy, instead of the two-body energy, is used as a parameter. This has been shown by Stiefel and Scheifele (ref. 8) to significantly improve the accuracy and stability of the solutions. The KS method, which has ten differential equations, can be specialized for elliptical orbits in which case the eccentric anomaly becomes the independent variable. Variation of parameters applied to the integration constants of the four dimensional harmonic oscillator

provides eight element differential equations. Two additional element equations come from the perturbed frequency ω (based on the total energy) and an element τ for the perturbed time.

The Burdet elements have been modified by Bond (ref. 9) so that they too contain the total energy element. Both element sets (KS and Burdet-Bond) have proven to be extremely accurate, stable, and yet have concise formulations. The two methods, however, are not well suited for analytical solutions.

Recently, a number of canonical element sets have been developed (refs. 10, 11, and 12) which incorporate a total energy element in an extended phase space. They have eight canonical dependent variables with an independent variable other than time. Two of the sets, DSϕ and DSu, are similar to the Delaunay elements and have the true and eccentric anomaly, respectively, as their independent variable. These sets have singularities for small eccentricities and inclinations. They have been transformed to Poincare' type elements, PSϕ and PSu, to remove the singularities. Unlike the classical elements, no iteration of Kepler's equation is required. All of these "extended phase space" sets have been shown to be as accurate and efficient as the KS set, but are not as concise in their formulation. Because they are canonical sets, they are more readily adopted to analytical perturbation theory.

1.2.4 Choosing a formulation.- In examining the different element formulations, one finds a number of characteristics which are considered desirable for use in a numerical orbit prediction program.

a. The elements should vary slowly and smoothly as a function of the independent variable.

b. The elements should always be defined for elliptical orbits.

c. The independent variable should be the true or eccentric anomaly, allowing for analytical step size control.

d. The energy element should include the total energy.

e. The formulation should require no iteration of Kepler's equation during the integration procedure.

Only the KS, Burdet-Bond, PSϕ and PSu elements of the total energy class exhibit all of these characteristics. Indeed, a wide range of experiments have consistently shown that the total energy formulations, when compared to the more classical formulations, are faster, far more stable, and yield more accurate results, while requiring very little (if any) more computer code (ref. 13 and 14). Two of these four sets, KS and PSϕ, were chosen for further testing and comparisons. The results and conclusions from the numerical experiments are discussed in section 1.4. An additional

objective was to match a numerical integration method to these two formulations. Several numerical integrators are discussed in the next section.

1.3 Numerical Integrators

Given the differential equations and initial conditions, one may employ finite calculus to numerically integrate the differential equations, giving the solution as a function of the independent variable and initial conditions. Two classes of integration methods will be discussed in this section:

a. Runge-Kutta (single-step) formulas

b. Adams (multistep) formulas

The major difference between these two classes is that the single step methods develop the solution over one step, requiring no previous information on the solution. The multistep formulas require a sequence of values of the derivatives in order to advance the solution one step. If the derivatives vary slowly and smoothly from step to step, then both classes perform well. If the derivatives become erratic or impulsive, the single step methods, with step size control, are preferred. Step size control with the multistep method is generally not possible.

Note that a step size control procedure that is built into an integrator is called "numerical" step size control. Compare this to the "analytical" step size control that is introduced in section 1.2.

1.3.1 Adams formula.- The classical Adams method is an example of a multistep formula. It uses the Adams-Bashforth formula (predictor) and the Adams-Moulton formula (corrector) to obtain the solution. A complete discussion of this method is given by Henrici (ref. 15).

The solution is extrapolated one step forward by applying the predictor formula. The derivative is then evaluated with the predicted solution and a corrected solution is obtained from the corrector formula. This classical predict-correct type of algorithm is not well suited for variable-step applications. Therefore, only fixed-step Adams integrators are included in this study. A truncation error estimate is available and can be used to determine the best step size.

Consider a vector that is defined by the first-order vector differential equation

$$\frac{d\vec{y}}{dx} = \vec{f}(x,y)$$

where x is the independent variable. Also define

$$x_j = x_o + jh$$

$$\vec{y}_j = \vec{y}(x_j)$$

$$\vec{f}_j = \vec{f}(x_j, \vec{y}_j)$$

The predictor and corrector formulas are

$$\vec{y}^{p}_{n+1} = \vec{y}_n + h \sum_{k=0}^{N} P_k \vec{f}_{n+k-N}$$

$$\vec{y}^{c}_{n+1} = \vec{y}_n + h \sum_{k=0}^{N} C_k \vec{f}_{n+k-N+1}$$

where $N+1$ is the order of both formulas.

Observe that the corrector formula is an implicit equation since $\vec{f}_{n+1}$ depends on $\vec{y}_{n+1}$. Usually, one iteration is sufficient for solving the equation. The coefficients P_k C_k are functions of the order of the formula. These coefficients may be computed recursively for any given order before the integration is initiated. For this reason the Adams method is sometimes called a "variable order" method.

The truncation error of the corrected solution is given by

$$\vec{T}_{n+1} = K_n \left(\vec{y}^{p}_{n+1} - \vec{y}^{c}_{n+1} \right)$$

where K_n is a function of only the order.

The first $N+1$ values of $\vec{f}_i$ are required to start the integration. In the numerical examples in Section 1.4, an eighth order RK formula was used to start the Adams integration.

1.3.2 Runge-Kutta formulas.- Runge-Kutta (RK) formulas fall in the class of single-step integration formulas. That is, they are self-starting. In general, an RK formula can be written as

$$\vec{y}_{n+1} = \vec{y}_n + \sum_{i=1}^{v} W_i \vec{K}_i$$

where W_i are weighting coefficients, v is the number of function evaluations required at each step and K_i is defined as

$$\vec{K}_i = h\vec{f}\left(x_n + C_i h,\ \vec{y}_n + \sum_{j=1}^{i-1} A_{ij}\vec{K}_j\right).$$

Equations of condition for W_i, C_i and A_{ij} are found by expanding the RK formula in a Taylor series. Solution of these equations provides the numerical values of the coefficients. To, date, however, there is no simple manner to obtain values of these coefficients for any order. A good discussion on RK methods is contained in reference 16.

A short description of five different RK formulas is given in the following subsections. A list is given below showing the number of "function calls" (NFC) that are required at each step by the various RK formulas. A function call is one evaluation of the differential equations.

RK formula	NFC per step
RK4	4
RKF45	6
RK45	6
RKS8	10
RK78	13

1.3.2.1 Classical fourth-order formula: The classical fourth-order formula (RK4) is

$$\vec{y}_{n+1} = \vec{y}_n + \frac{1}{6}\left(\vec{K}_1 + 2\vec{K}_2 + 2\vec{K}_3 + \vec{K}_4\right)$$

$$\vec{K}_1 = h\vec{f}(x_n, y_n)$$

$$\vec{K}_2 = h\vec{f}\left(x_n + \frac{1}{2}h,\ \vec{y}_n + \frac{1}{2}\vec{K}_1\right)$$

$$\vec{K}_3 = h\vec{f}\left(x_n + \frac{1}{2}h,\ \vec{y}_n + \frac{1}{2}\vec{K}_2\right)$$

$$\vec{K}_4 = h\vec{f}\left(x_n + h,\ y_n + \vec{K}_3\right)$$

It is very popular and quite efficient. However, when compared to other available RK formulas, it has the following disadvantages.

a. No step size control.

b. Less efficient for accurate integration.

Its chief advantage is the small computer storage requirement.

1.3.2.2 Fehlberg's formulas: Fehlberg's RK formulas overcome the two disadvantages mentioned above. His formulas contain an automatic truncation error estimate and are available in orders one through eight (refs. 17 and 18). Reference 19 contains a discussion of the error propagation, as well as the coefficients for each RK-Fehlberg formula. A fifth order version (RKF45) and an eighth order version (RK78) have been tested.

1.3.2.3 Bettis' improved formula: New versions of Fehlberg's formulas are being developed by Dale Bettis at the University of Texas, Austin. He uses a Davidon optimization scheme to compute new RK coefficients that minimize the truncation error. The expression for the truncation error is known as an analytical function of the coefficients. Therefore, the optimized coefficients apply to any set of differential equations and, in effect, raise the order of the formula (ref. 20).

Dr. Bettis has made available to the Mission Planning and Analysis Division (MPAD) his optimal version of RKF45, which will be referred to here as RK45. There is no increase in computer run time or storage over that for RKF45 since the algorithm is the same.

1.3.2.4 Shanks formula: An additional RK formula developed by Shanks (ref. 21) has also been tested. It was chosen since it was of high order and has been shown by other investigators (ref. 22) to have accuracy comparable to that of Fehlberg's formulas.

Shanks attempted to minimize the number of function evaluations per step for a given order. The formula tested here (RKS8) is approximately an eighth-order formula and requires only 10 function evaluations per step (RKF78 requires 13) but it contains no step size control. Therefore, it is expected that RKS8 will be more efficient than RKF78 when a constant step is desirable, such as for circular orbits. The reverse situation is expected for very elliptical orbits.

1.3.3 General remarks.- For the special case of orbital motion, the right-hand side of the differential equations are usually smooth functions of the dependent variable. In this regard, the Adams formulas are expected to be more efficient than the Runge-Kutta formulas. Elliptical orbits may, however, require the variable step size option of the RK formulas.

The required order of an integrator for a given accuracy depends on the formulation of the differential equations. A method such as the Cowell formulation requires a high order integrator to obtain satisfactory results. But, a method such as the KS formulation is somewhat insensitive to the order of the integrator (see section 1.4), i.e., all integrators perform about the same.

Although high order integrators are usually more accurate they are also less stable (ref. 22). Thus, in choosing the integrator one must find a happy medium where the order is large enough for reasonable accuracies but small enough not to introduce instabilities.

1.4 Formulation-Integrator Combinations

When building a numerical orbit prediction program, it is desirable to choose the formulation and integration method that best satisy the requirements discussed in section 1.1 (Force model requirements are discussed in section 2.0). The discussion in this section concerns the choice of these two important components and relies on both theoretical considerations and numerical experiments. Use was made of the results and experience of prior investigators to eliminate some methods and limit the number of possible combinations.

Several different problems of orbit prediction were chosen for the numerical experiments. The orbits chosen are important for shuttle orbiter and payload missions. Also, they demonstrate the different qualities of the differential equation formulation - numerical integration (DE - NI) combinations. A thorough discussion of the comparison is contained in reference 23. The following gives a summary and the conclusions.

1.4.1 Formulations investigated.- The discussion in section 1.2 concluded that there are four available element sets (KS, Burdet-Bond, PSϕ, PSu) that have significant advantages over all the rest. These four are in the class of "total energy elements" and each is based on an independent variable different from time. It was decided to choose two of these for further testing and evaluation.

In choosing between the four total energy element sets, several considerations were made. First, PSϕ has true anomaly as the independent variable, the remaining three have eccentric anomaly. Thus, PSϕ was chosen for further testing in order to determine the advantage of the step spacing (fig. 1) of the true anomaly. For orbits that are strongly perturbed by the geopotential and drag, PSϕ should have an advantage.

KS was chosen from among PSu and Burdet-Bond because (compared to PSu) it has a concise formulation and it has fewer elements than Burdet-Bond (10 versus 13). Numerical experiments and theoretical analyses of Bond (refs. 10 and 24) indicate that the PSu has a slight advantage in long term stability. However, this

does not seem to be significant enough (for most applications of orbit predictors) to offset the value of a concise formulation.

1.4.2 Numerical integration methods investigated.- Graf (ref. 13) investigated a number of different numerical integrators with the Cowell and KS formulations. From the conclusions of that report it was determined that four integrators had advantages that warranted a thorough investigation with the KS and PSϕ formulations. A short description of these integrators and the reasons why they were chosen are listed below:

a. AD9 - This is an Adams (multistep) method of ninth order which evaluates the derivative once per step. This fixed step method proved to be very efficient with the KS method even for eccentric orbits.

b. RK4 - This is the classical fourth order Runge-Kutta (single-step) method which requires four derivative evaluations per step. Even though this is a simple, low order method it proved efficient with the KS method.

c. RK45 - This is the fifth order Runge-Kutta method with the option of step size control. It requires six derivative evaluations per step and uses Bettis's optimized coefficients because of their proven accuracy (ref. 20). This method was chosen mainly because of its powerful step size control.

d. RK78 - This is the eighth order Runge-Kutta-Fehlberg method that requires 13 derivative evaluations per step. It does have the option of step size control. It was chosen for its efficiency for stringent accuracy requirements.

1.4.3 Comparisons based on storage and cycle time.- In comparing KS and PSϕ one might argue that the KS formulation has a clear advantage because it is so concise. Certainly, if one compares storage one finds that PSϕ equations require 100 percent more computer storage than KS equations. However, this is not quite a fair comparison. One should always compare formulations by the percentage of the formulation storage to the storage required by the total orbit prediction algorithm which includes the force model and numerical integrator. Thus with a force model which adequately represents the forces on a satellite about the Earth and with an integrator such AD9, KS composes 13 percent of the total storage and PSϕ only 23 percent. Therefore, the impact of the PSϕ additional overhead is not as large as it might first appear, but still should be considered for very stringent storage requirements.

We define cycle time as the time required for one evaluation of the derivatives of an element set. Certainly KS will have a smaller cycle time than PSϕ. But for accurate predictions, a large force model is required and thus most of the time evaluating

the derivatives is spent in the force model. Thus one finds that the cycle time for PSϕ is only 6 percent more than the KS cycle time.

One can only conclude that, for accurate orbit predictions where a large force model is required, the overhead of PSϕ is negligible except for very stringent storage and cycle time requirements.

1.4.4 Comparisons based on accuracy and execution time.- The four integration methods and the KS and PSϕ formulations have been programed in double precision on the Univac 1110 (ref. 25). The results of the various comparisons are displayed in graphical form (figs. 2(a) through 2(d)). The bottom scale in each graph is the execution time (cpu time) in seconds and the left-hand scale is the accuracy defined as

$$\delta = -\log_{10}\left(\frac{\Delta R}{R}\right)$$

where

ΔR is the position vector difference magnitude between the test and reference solutions at the final time.

R is the position magnitude of the reference solution which is accurate to 10 digits.

Note that the cpu time was varied by taking successively smaller step sizes or tolerance criteria in each of the NI - DE combinations. Methods whose curves lie above and to the left are therefore considered the most efficient.

Again, one should refer to reference 23 for a more detailed description of these numerical comparisons, graphical displays, and conclusions.

1.4.4.1 Near Earth orbit: This test case has the following initial conditions

h_a = 278 km $\quad$ I = 28.4° $\quad$ Epoch of Jan. 1, 1975

h_p = 167 $\quad$ $\omega = \Omega = M = 0°$

The force model includes air drag and an eighth order, eighth degree geopotential model. The final time of integration is t_f = 2.0 days which is about 32 revolutions.

Results:

The KS and PS performed about the same, which could be expected for this near circular orbit. All the Runge-Kutta methods performed about the same and both formulations appear to be insensitive to the order of the integrator. In both formulations,

the AD9 method was slightly more efficient than the RK methods. This too could be expected since the forces vary slowly and are very smooth in this case. Figure 2(a) displays the efficiency curve of the KS and PS combinations with AD9 and RK45.

1.4.4.2 Geosynchronous orbit: This test case has the following initial conditions

$h_a = h_p = 35862$ km Epoch of Jan. 1, 1975

$\omega = \Omega = M = 0.0^\circ$ $I = 0.0^\circ$

$t_f = 100$ days = 100 revolutions

The force model includes the Sun and Moon perturbations and a fourth order, fourth degree geopotential model.

Results:

Again, the KS and PS methods performed almost the same. For accuracies of $5<\delta<6$ or about 100 to 1000 meters, the RK4, RK45 and AD9 are almost equivalent. For slightly more stringent accuracies, the AD9 integrator is most efficient in either formulation. The RK78 fails to be competitive except for very stringent accuracies of $\delta>7$ (less than 1 meter). Figure 2(b) displays the curves of the KS and PS combinations with AD9 and RK4.

1.4.4.3 Elliptical transfer orbit: The initial conditions of this case are

$h_p = 200$ km $I = 30.0^\circ$

$h_a = 35862$ km $\omega = \Omega = M = 0.0^\circ$ Epoch of Jan. 1, 1975

$t_f = 2.0$ days $\simeq 4$ revs

The force model includes drag, an eighth order, eighth degree geopotential and Sun-Moon perturbations. Note that in this case the forces at perigee are much stronger than those at apogee.

Results:

In this case the PSϕ formulation proved to be much more efficient than KS, regardless of integration method. This was expected since PSϕ uses the true anomaly as the independent variable. Fixed step AD9 combination with PSϕ showed the highest efficiency. But the RK45 with its excellent step size control could be used with either KS or PSϕ for competitive efficiencies. The RK78 showed to be inefficient again except for stringent accuracies. Also the fixed step methods AD9 and RK4 fared poorly when used with the KS formulation. This is because the KS independent variable (eccentric anomaly) is not well suited for this case. Figure 2(c) displays the KS and PS combinations with AD9 and RK45. Note the

large difference between the AD9 combinations but small difference between the RK45 combinations.

1.4.4.4 Highly eccentric orbit: The initial conditions of this case are

h_p = 425 km $I = 30^\circ$.

h_a = 258,903 km $\omega = \Omega = M = 0.0^\circ$ Epoch of Jan. 1, 1975

$e = 0.95$.

The force model includes drag, an 18th order geopotential and the Sun-Moon perturbations. The final time of integration is t_f =

50 days ~ 8.6 revolutions. Note in this case the perturbation forces are equally strong at perigee and at apogee.

Results:

The KS formulation showed to be the stronger formulation in this case which is again to be expected since the eccentric anomaly as independent variable is better suited for this highly eccentric orbit. The RK45-KS combination was the most efficient but one could use the RK45-PS and even the fixed step AD9-KS combination without much loss in efficiency. The RK78 integrator appeared to have stability problems and its step size control did not perform well. Since the true anomaly is not well suited with this case, the fixed step methods AD9 and RK4 did not do well with PSϕ. Figure 2(d) shows the accuracy curves of the PSϕ and KS formulations with RK45 and AD9.

1.4.5 Conclusions from comparisons.- It was concluded from previous experiments that the PSϕ and KS formulations possess most or all of the attributes listed in the introduction. The comparisons have shown the KS method does have a slight advantage in relation to storage requirements and cycle time. Results from the numerical studies show that both methods are equally powerful for circular orbit cases but differences between the two formulations become apparent for more eccentric orbits.

It is recommended for circular orbits with slowly varying forces (such as the two cases that were examined) that the AD9 integrator be used with either the KS or PSϕ formulation for the most efficient results. However, the RK4 and RK45 integrators may also be used with little loss in efficiency. If the force model includes discontinuous forces such as venting, one may find that a low order single-step method such as RK4 to be more adequate.

In the case of eccentric orbits where the perturbing forces are much stronger at perigee than at apogee (such as the elliptic transfer orbit), the PSϕ formulation should be used. For best results the AD9 integrator is recommmended. However, an integrator

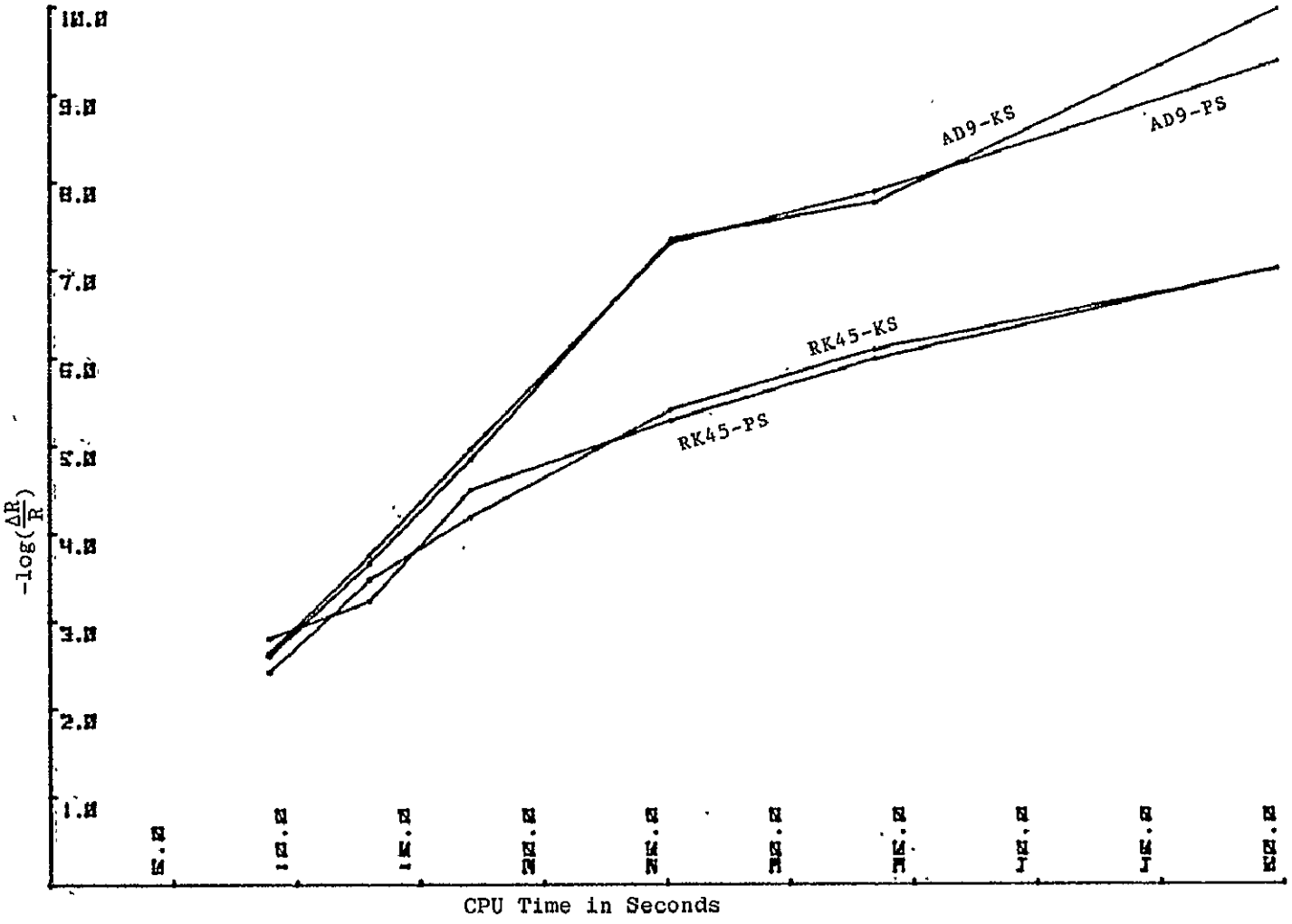

(a) Near-Earth orbit.

Figure 2.- Numerical efficiency curves.

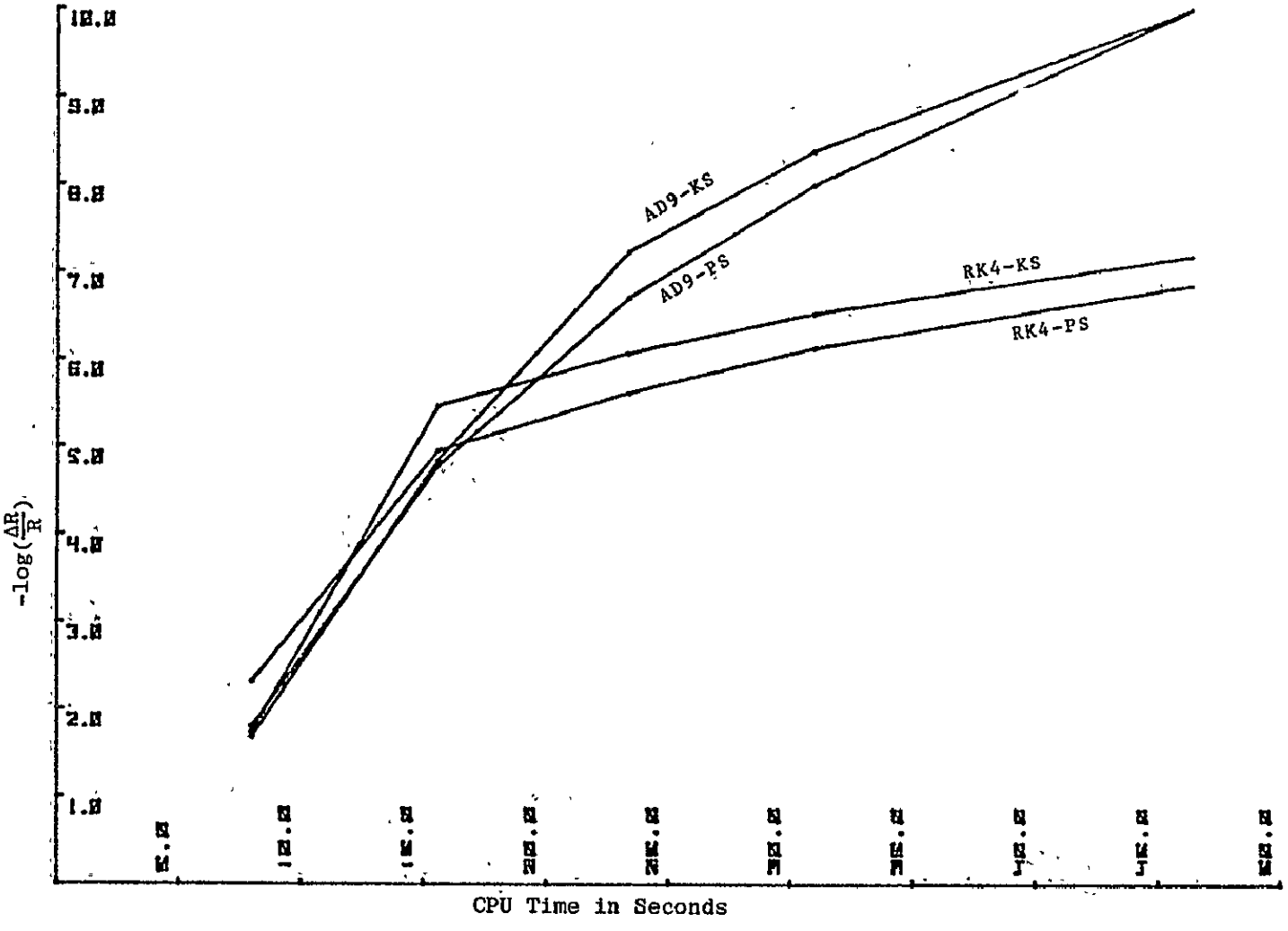

(b) Geosynchronous orbit.

Figure 2.- Continued.

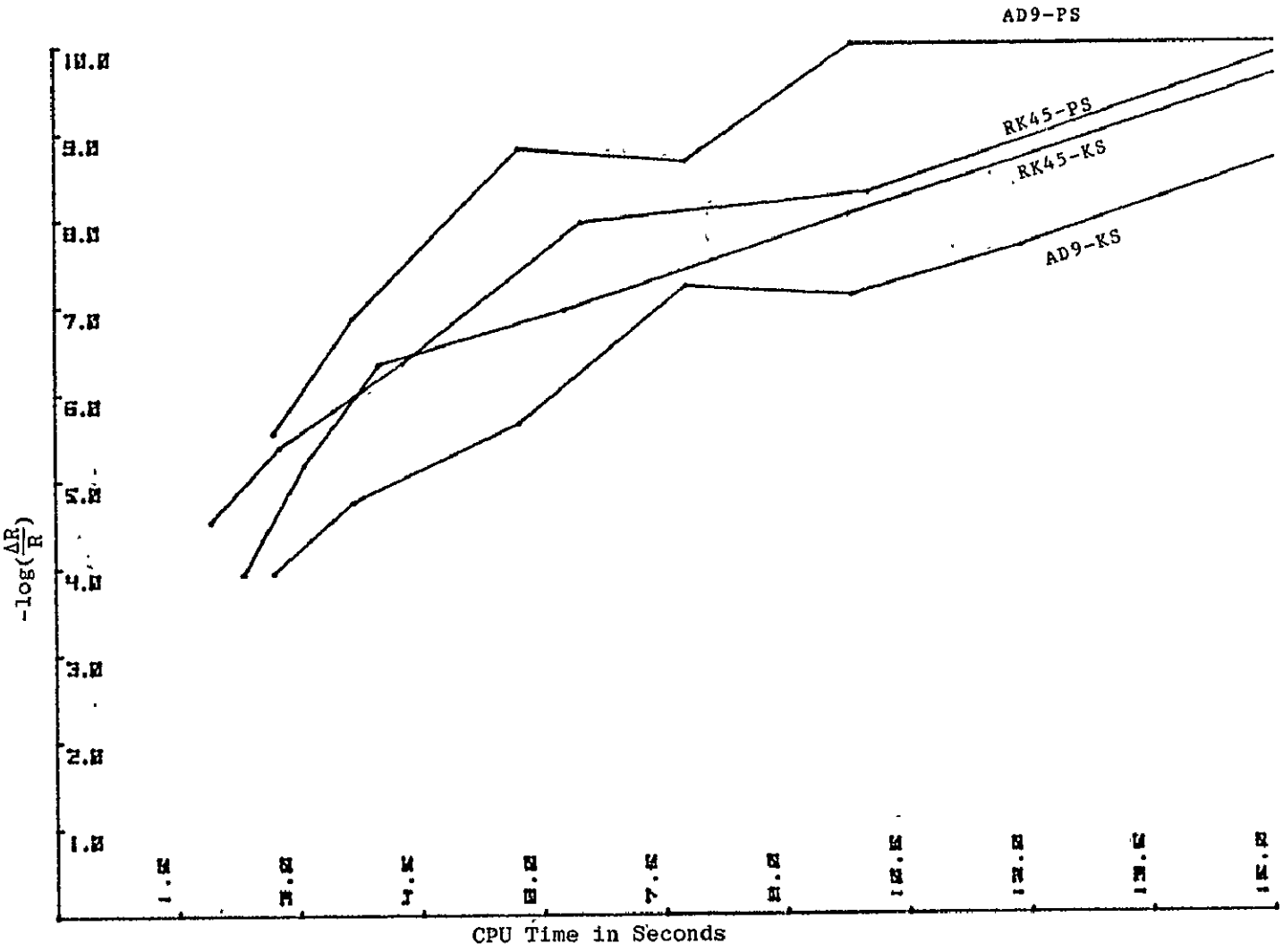

(c) Elliptic transfer orbit.

Figure 2.- Continued.

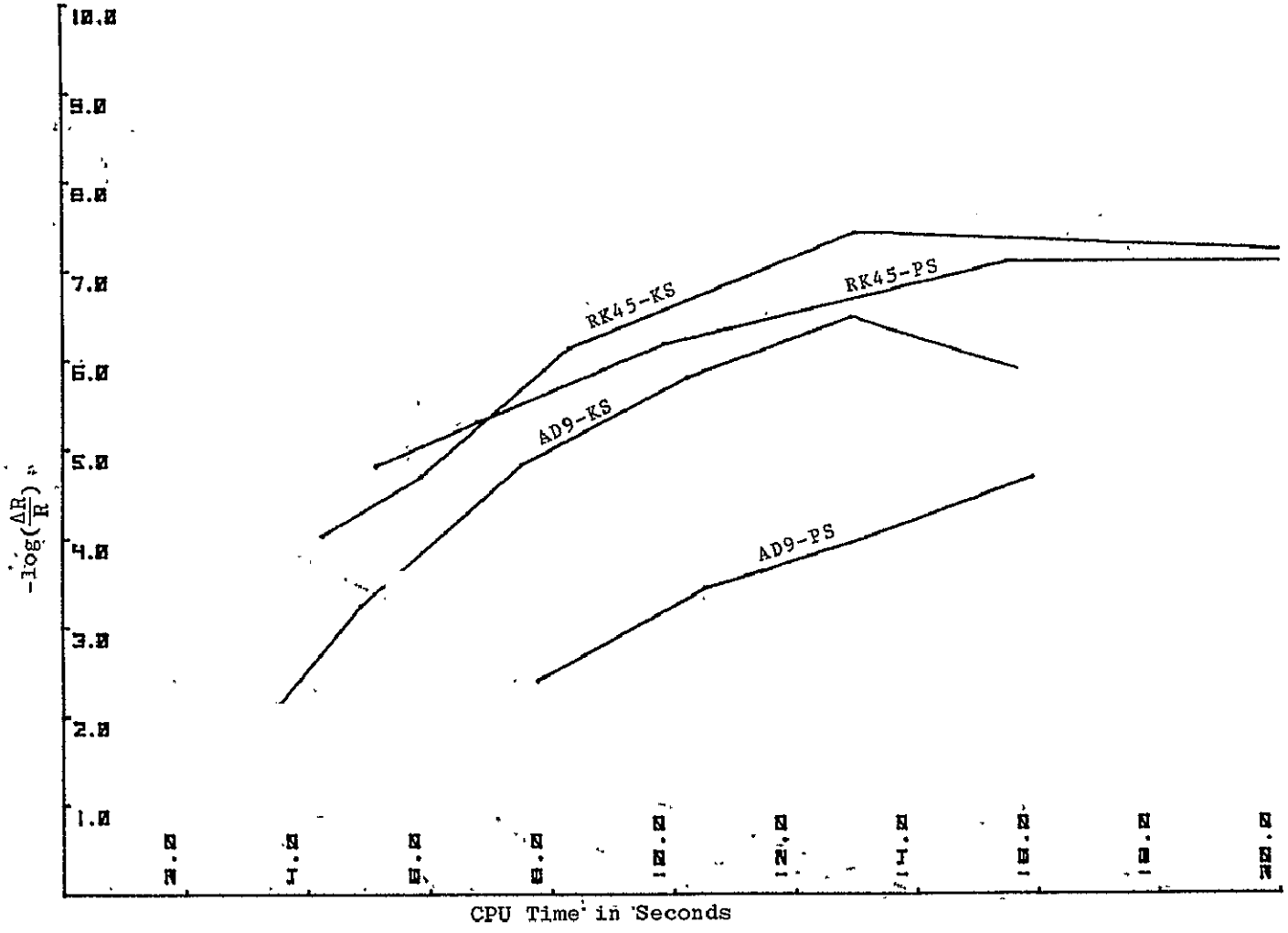

(d) Highly eccentric orbit.

Figure 2.- Concluded.

with good step size control such as RK45 may be used with KS formulation for competitive results.

For highly eccentric orbits, where the perturbing forces are important at both perigee and apogee, the KS formulation is best. Although the KS formulation has an analytic step size control that is suited for this case, the method produces the most efficient results with the help of the excellent RK45 numerical step size control. Adequate results may also be obtained from the RK45-PS combination.

From the study, it appears there is no clear cut "winner" between KS and PSϕ formulations. Certainly, both methods are very powerful and should be considered as the leading contenders for numerical orbit prediction algorithms. The AD9 method certainly is the best integrator when the analytical step size control is adequate but the RK45 becomes powerful when additional help is needed for step size control.

1.5 Analytical Solution Methods

Whereas the numerical methods that were discussed in the previous sections develop the solution in discrete steps, analytical methods produce the solution in the form of finite mathematical expressions. These expressions contain explicitly the dependent variable. Numerical evaluation of these expressions provides the position and velocity of the satellite at a given time.

An analytical solution can be thought of as a "one step" method. When used for orbit prediction, the computation cost to obtain the state is always the same, regardless of the prediction interval. Typical computation time is less than one second.

Analytical solutions to the J_2 (oblateness) problem have been established in the DS-elements (ref. 11) and PS-elements (ref. 12). An orbit prediction program (ANALYT) based on the DS analytical solution has been developed and is documented in reference 26. Numerical experiments contained in reference 26 show that ANALYT solutions of the J_2 problem have errors on the order of a few meters, so long as the eccentricity is larger than 0.01. In addition, this error remains constant over several hundred revolutions (ref. 11).

Additional testing of the ANALYT program was carried out in reference 27. The reference trajectories were obtained from the KSFAST program (ref. 28), using an 18th order, 18th degree geopotential model plus atmospheric drag. It was found that the program gives good results for those orbits where drag is not so

important; i.e., height of perigee is above 700 km. Position errors for a prediction of 60 revolutions was on the order of a few kilometers.

1.6 Multirevolution Methods

A seminumerical orbit prediction method has been developed, based on the multirevolution integration technique. The method makes use of the fact that the orbital motion of a satellite is nearly periodic from revolution to revolution, as measured from some orbital reference point such as perigee. The algorithm can extrapolate the satellite's orbital elements many revolutions ahead, thereby saving much computation time. Typical applications are for lifetime studies, orbit stability analyses and reference trajectories.

Let $\vec{y}_\rho$ be the osculating elements at a prespecified orbital reference point. Then the multirevolution method solves the folowing first order difference equation,

$$\vec{y}_{\rho+1} - \vec{y}_\rho = \vec{f}(\vec{y}_\rho, \rho)$$

where ρ is the revolution number. The above equation results from the finite change in the elements over one revolution, measured from the reference point. This change may be computed by a numerical integration of the equations of motion, with the use of $\vec{y}_\rho$ as initial conditions. Since ρ will have integer values only, the elements $\vec{y}$ are known at discrete points of a continuous independent variable, forming a grid of equal intervals. The multirevolution method provides the solution of the difference equation at points separated by M grid points, where M is the multirevolution "stepsize". The computed solution is then established on a large grid, each interval of which contains M subintervals.

The multirevolution formula is written as

$$\vec{y}_{(n+1)M} = \vec{y}_{nM} + M \sum_{j=o}^{N} \alpha_j^p \nabla^{*j} \vec{f}_{(n+p)M}$$

$$p = 0, 1$$

The subscripted expressions on $\vec{y}$ and $\vec{f}$ refer to the revolution number. $p = 0$ gives a predictor formula and $p = 1$ a corrector formula. n is the step number. The backward differences ∇^* are defined as

$$\nabla^{*j+1}\vec{f}_{nM} = \nabla^{*j}\vec{f}_{nM} - \nabla^{*j}\vec{f}_{(n-1)M}$$

The coefficients α_j^p are polynomials in $\frac{1}{M}$. The above formula is very similar to the Adams formula (section 1.3.1). Further theoretical details of the multirevolution algorithm are given in references 29 and 30.

An orbit prediction program KSMULT based on the multirevolution algorithm has been developed and is documented in reference 31. The KS elements are used for extrapolation and the differences are computed by the KSFAST program. Therefore, all of the input/output and force model options of KSFAST are available to KSMULT.

Numerical evaluations of KSMULT have been carried out (ref. 32). The purpose was to determine the optimum values for the order N and stepsize M, when the multirevolution algorithm is applied to near Earth orbits. The initial parameters of the orbit investigated were:

altitude	296 km
eccentricity	0
inclination	30°
period	90.4 min

Perturbations included an 18th order zonal geopotential model plus air drag (Jacchia density model). Results are shown in table I(a) and (b) for prediction intervals of 125 days and 165 days, respectively.

TABLE I.- KSMULT TEST RUNS

(a) Prediction Interval = 125 days

N	M	ΔR	cpu time	Savings factor
6	16	2.0 km	162 sec	6.8
6	24	11.1	118	9.3
8	16	.8	169	6.5
10	16	8.9	175	6.3

TABLE I.- Concluded

(b) Prediction Interval = 165 days

N	M	ΔR	cpu time	Savings factor
6	16	9.1 km	204 sec	7.1
8	16	1.6	211 sec	6.9

Notes:

1. The reference solutions were obtained from KSFAST. ΔR is the vector magnitude of the position difference in the KSMULT and KSFAST solutions. This is primarily a downrange error.

2. The errors in these predictions are on the order of a few kilometers. This is less than the expected errors due to force model inaccuracies (see Section 2.0).

3. Ratios of KSFAST cpu time are shown in the column under "Savings Factor." This gives an indication of the savings to be realized with KSMULT. Note that the total KSMULT runtime for precision computations of 2628 revolutions (table 1(b)) is only about 3 1/2 minutes.

4. According to these results (and addtional results in reference 32), M=16 and N=8 are the optimum values for near Earth orbits.

5. This particular orbit decayed at 170 days. During the final stages of the decay, the orbital elements change rapidly and multirevolution is no longer the appropriate numerical integration method. The program can then switch to KSFAST for computation of the final few revolutions.

An additional multirevolution program STEPR has been built, based on the routines in the general orbit prediction program (GOPP) (ref. 25). STEPR is described and documented in reference 33. All of the element sets (KS, PSϕ, PSU, DSϕ, DSU, Cowell) and integration methods (Adams, RK4, RK45, RK78) that are contained in GOPP are available to the multirevolution algorithm. STEPR represents a new concept for orbit prediction programs: any orbit predictor can have the multirevolution technique as an additional option, thereby making it several times more efficient for long predictions.

STEPR has been used as a prototype program and tool for the following investigations:

a. Determine the best set of total energy elements and numerical integration methods for applying multirevolution to a variety of orbit types (ref. 33).

b. Determine the accuracy limitations of the multirevolution method (ref. 33).

c. Study the orbital motion of the proposed solar power satellite over a time span of 30 years.

d. Lifetime studies of near Earth satellite.

e. Evaluation of refinements to the multirevolution algorithm.

1.7 Concluding Remarks

A discussion has been given on several new methods for orbit prediction. Included are numerical, analytical and seminumerical methods. Comparison test results have been summarized. Suggestions have been made on the use of the new methods for production applications.

For numerical orbit prediction methods, it was found that the "total energy" element formulations produced more efficient results when compared to classical formulations. A comparison between the two total energy formulations, KS and PSϕ, showed no major difference for circular orbits. However, for eccentric orbits, differences become apparent because the formulations have different independent variables. It was found that, if the independent variable was suited for a particular orbit, then more efficient results could be realized. Several numerical integration methods were investigated in conjunction with KS and PSϕ formulations. For circular orbits, all integrators, including the fourth order Runge-Kutta (RK4), proved to be competitive. In eccentric orbits, it was seen that a fixed step Adams method (AD9) was the most efficient integrator, if the formulation's independent variable was suited for the orbit. Otherwise, a fifth order Runge-Kutta (RK45) with its excellent step size control proved more efficient.

Accurate and concise analytical solutions have been obtained through the use of the canonical total energy elements. The solutions require a negligible amount of computer time and are feasible for orbit predictions if the unmodeled forces are small.

For long term integration, it was found that a seminumerical orbit prediction method, based on the multirevolution technique, results in a large savings in computation time. Yet the errors in the solution are still smaller than the predicted errors due to force model inaccuracies. This versatile method may be applied to any numerical orbit prediction technique.

2.0 MATHEMATICAL MODELS OF THE PERTURBING FORCES

2.1 Introduction

The environment of an Earth satellite includes a variety of forces and effects that actively perturb its orbit from the idealized two-body motion. This part of the report will investigate these forces and their impact on the accuracy and cost of orbit predictions.

A computer program for numerical orbit prediction usually has the four basic modules:

a. Input/output and initialization
b. Formulation of the satellite differential equations
c. Numerical integration routine
d. Mathematical model of the perturbing forces.

Under consideration here are the various models that are available to make up the fourth module.

Analytical orbit prediction methods are somewhat diffferent from the numerical methods in that they usually do not exist as a combination of modules. The formulation, integration routine and force model are contained in the same set of equations. If necessary, they can be separately defined. However, it is not the intention to discuss the solution method in this section. The important thing is that each orbit prediction method (numerical or analytical) consists, in some way, of the above modules. In particular, the force model, once it is defined, plays a large part toward determining the applicability of the resulting computer program.

Accuracy is of fundamental importance in any computer program. Sources of possible error in predicting satellite trajectories are:

a. Roundoff and truncation errors,
b. Inaccurate initial position and velocity, and
c. Inaccurate models of the perturbing accelerations.

Roundoff errors result from the fixed word length that exists in all computing machines. That is, only a limited number of digits are carried throughout the arithmetic operations. Algorithms that require more arithmetic operations will be more affected by roundoff errors. From this point of view, the fewer numerical integration steps needed to compute a trajectory, the better. Also, roundoff errors are very machine dependent because of different word sizes and methods of rounding.

Truncation errors are due to the finite difference calculus that is carried out on a computer. Continuous functions are "discretized" and computed at finite intervals of the dependent and independent variables. This is mathematically equivalent to

truncating the infinite Taylor series expression, hence the term "truncation error." With numerical integration methods, the higher order formulas have agreement to more terms in the Taylor series and less truncation error. Thus, they are generally more accurate. The accuracy is usually controlled to be within prespecified bounds at each step, in order to limit accumulation of truncation errors.

Section 1.0 discussed truncation and roundoff errors that result from a variety of methods; i.e., the numerical accuracy in solving the programed equations.

The second error source, initial position and velocity errors, is related to physical accuracy because, typically, they are obtained from an orbit determination program that has limited accuracy (due to roundoff and truncation errors, tracking errors, etc.). When input into an orbit prediction program, their slight deviation from the exact values can cause an appreciable deviation between the real and computed trajectories. These initialization errors are not studied in detail in this report. If expected values of the initial errors are known, their importance relative to roundoff, truncation and force model errors can be determined.

This section is concerned with the third error source, inaccurate and/or incomplete model of perturbing forces. Generally, the models differ in their accuracy and complexity. They must all ultimately be based on empirical mathematical formulas and observational data. The physical constants (such as mean radius of the Earth, gravitational constant, air drag coefficient, etc.) are determined from such data and are necessarily limited in accuracy, due to observational inaccuracies and roundoff in computations. It is not the intention of this study to verify or refine the agreement to observations. Instead, several existing models are systematically compared to determine their efficiency and accuracy when used in an orbit prediction program. Efficiency is determined by a model's computer execution time and storage. It is desired to find the least complex force model that delivers a required accuracy in a computed trajectory.

A necessary condition for using numerical orbit prediction programs to study force model effects is that the numerical errors be less than the force model errors to be studied. The analysis and comparisons carried out in section 1.0 prove that this condition is satisfied in the case of the programs (KSFAST and GOPP) that are used in this study.

Typical forces affecting the motion of an Earth satellite are:

a. Atmospheric drag
b. Nonsphericity of the Earth
c. Sun and Moon gravity
d. Reference coordinate system inaccuracies
e. Solar radiation pressure

f. Uncoupled attitude maneuvers
g. Vehicle venting

An indepth discussion of the first four are given in this report. Density models of the upper atmosphere are discussed in section 2.2. The USSR-AST.P and Jacchia models are compared. A new dynamical (time dependent) density model is presented and tested against the Jacchia model. In section 2.3, an analytical Sun-Moon ephemeris model is described and compared to the stored ephemeris of the JPL tape. The geopotential model is discussed in section 2.4. It is shown how the different terms in the geopotential expression affect the trajectory. Suggestions are made on a simplified geopotential model. Section 2.5 concerns the effects of noninertial coordinate systems on the trajectory. Finally, recommendations are given in section 2.6 on the correct force models to be used when predicting the following types of trajectories:

Shuttle-type near Earth circular orbits

Elliptical transfer orbits ($e \cong 0.7$)

Geosynchronous orbits

Near Earth orbit lifetime problems

The complexity of the various forces, and the diversity of satellite shapes and orbits, makes it very difficult to consider all possible perturbations. This study has, of necessity, been somewhat limited in scope. The last three of the above mentioned affects will not be discussed. However, it will be made clear in each subsection as to the scope and limitations of each force model studied.

2.2 Atmospheric Density Models

Atmospheric drag is an important perturbation on the orbits of near Earth satellites, such as the shuttle orbiter. The drag force model includes two effects:

a. The aerodynamic interaction of the satellite with the upper atmosphere, and

b. The variable atmospheric density.

The first depends on vehicle characteristics; i.e., the satellite's shape and body attitude. The second depends on altitude, time of day, geographical position and date.

The acceleration $\vec{a}$ due to drag is based on the empirical equation

$$\vec{a} = -\frac{1}{2} C_d \frac{\rho}{B} |\vec{v}| \vec{v} \qquad (2\text{-}1)$$

where ρ is the atmospheric density at the position of the satellite, $\vec{V}$ is the velocity magnitude and direction of the satellite relative to the atmosphere, and C_d is the drag coefficient. The ballistic number B is defined as the weight divided by the cross sectional area of the satellite.

It has been determined experimentally that the drag coefficient of a vehicle moving in a rarified atmosphere is approximately 2.2. Therefore, the studies described in this section have been based on

$$C_d = 2.2$$

The ballistic number depends, in general, on the angle between the vectors $\vec{V}$ and $\vec{\Omega}$, where $\vec{\Omega}$ is the body orientation vector. For the shuttle orbiter, B can vary between (approximately) 50 and 400 lbs/ft^2. For this study, an intermediate value of

B = 100 pounds per square foot

has been used throughout; i.e., B was held constant in all comparisons.

2.2.1 Description of the models.- The density at any point above the Earth's surface generally depends on altitude, time of day, and level of solar activity. These variations, if incorrectly modeled, may result in inaccurate orbit predictions for satellites that are near the Earth. Nondynamic models such as the 1962 U.S. Standard Atmosphere do not include the time dependence and solar activity effects. Four density models were investigated (refs. 34, 35, 36, and 37):

a. An analytical nondynamical model based on the 1962 U.S. Standard Atmosphere. This model is described in reference 38 and will be called the AMDB model. It uses exponential functions to describe the 1962 atmosphere. In a trajectory prediction program, it uses a negligible amount of computer storage and execution time.

b. The Jacchia model (ref. 39). This model is composed of two parts:

(1) The determination of the exospheric temperature as a function of position, time, and the solar and geomagnetic activity.

(2) The determination of density as a function of the exospheric temperature and altitude.

In addition to the solar and geomagnetic activity, the model contains semiannual and diurnal atmospheric variations. Empirical formulas based on these variations are used to obtain the exospheric temperature.

c. The USSR (Russian) model used in the Apollo-Soyuz Test Project (ASTP) mission. It includes the four effects mentioned in (b) above and is based on the tracking data of Cosmos satellites for the period from 1964 to 1970 inclusive. It is not as versatile as Jacchia's model since the solar radiation intensity data is assumed fixed for the year 1975 (ref. 40).

d. A new analytical model (AMDB*) which contains diurnal variations (refs. 36 and 37). In addition, it can be initialized to agree with Jacchia's model. It requires less computer storage and runtime than Jacchia or USSR.

The required input data for each model is as follows:

AMDB - satellite altitude above the Earth

Jacchia - satellite altitude above the Earth,

- position vector of the satellite relative to the Earth,
- position vector of the Sun relative to the Earth,
- Julian date of the satellite's state vector

Russian - satellite altitude above the Earth,

- position vector of the satellite relative to the Earth,
- position vector of the Sun relative to the Earth,
- number of hours from midnight December 31

AMDB* - satellite altitude above the Earth

- position vector of the satellite relative to the Earth,
- Julian date of the satellite's state vector

The AMDB* model was developed by Gus Babb (NASA/JSC), Stephen Starke (ACM) and Alan Mueller (ACM) when it became apparent that the three other models had significant deficiencies. The most notable were:

AMDB - The exponential formulas were not accurate enough. In some cases, this model gave no better results to orbit predictions than if air drag had been completely neglected.

Jacchia - This model involved large costs in terms of computer storage and execution time.

USSR - Poor results were obtained for epochs other than 1975. Also, it was grossly inaccurate at the lower altitudes (120 km).

2.2.2 Method of evaluation.- The purposes of this study are twofold: (1) determine the effects of atmospheric density variations on the path of a near Earth satellite, and (2) evaluate the various density models in terms of accuracy and efficiency.

It would be desirable to compare each model directly to the actual density of the upper atmosphere at a given position and time. This is not possible because direct density measurements are not available. In fact, the density is determined indirectly by its effect on satellite motions. This was the procedure used to develop the Jacchia and USSR models. Therefore, it need not be repeated here

Since both the Jacchia and USSR models were developed independently, and since both are based on satellite tracking data, a conservative estimate of their accuracy can be determined by comparing them to each other in epoch 1975. Output densities are compared in table II.

TABLE II.- DENSITY OUTPUT, JACCHIA VERSUS USSR

Altitude, km	Difference, percent
120	71.2
240	8.9
320	1.4
500	9.8

The large difference at 120 km is due to the inaccurate USSR model at lower altitudes. It therefore should not be used when the satellite's altitude is less than approximately 200 km.

Trajectory comparisons were made by examining the predicted position of a near Earth satellite (h_a = 220 km, h_p = 380 km). A complete geopotential model was used. Predicted position based on Jacchia and USSR density models are compared in Table III for epoch 1975.

TABLE III.- POSITON DIFFERENCE, JACCHIA VERSUS USSR

Prediction interval, days	Position difference, km
0.5	0.4
1.0	1.7
5.0	39.0

The Jacchia model is considered to be more complete than the USSR model, because it can be applied to the full range of altitudes and epochs (ref. 34). Also, it is in wide use at NASA/JSC. It was used, therefore, as the reference for these studies.

2.2.3 Effects of the Sun on the upper atmosphere.- In addition to the nearly exponential variation with altitude, the upper atmospheric density varies according to the time of day (diurnal), time of year (seasonal), and level of solar activity. The diurnal effect is a "bulge" on the atmosphere caused by solar heating of the sunlit side. A change in seasons causes the bulge to change latitudes.

It has been found that these three effects can cause a significant variation in the density at any point of altitude 500 000 feet or higher. This section shows the variation as a function of altitude of the diurnal and solar activity effects.

The Jacchia model was used to determine the atmospheric density at altitudes between 120 km and 600 km. Figure 3(a) shows how the density varies between these altitudes. The four curves show the difference between the atmosphere in sunlight and darkness, as well as the effect of solar intensity in 1970 and 1975. The Sun shadow curves show the diurnal effect. The reference density is $\rho_o = 1.225\ kg/m^3$.

The curves in figure 3(a) converge at about 500 000 feet (152 km). At this altitude and below there is good agreement between Jacchia and the AMDB exponential model.

More explicit details of the diurnal variations are shown in figure 3(b) where the density ratio function $-\ell n\ \rho/\rho_o$ is plotted against the Sun's hour angle. The daily variation is apparent.

To determine the effects of these variations, satellite orbit predictions were carried out using the Jacchia and AMDB models, and also for the case where air drag is neglected. The orbit conditions were the same as for the case in section 2.2.2. Positions in the orbit are compared against the Jacchia-based solution in table IV.

TABLE IV.- POSITION DIFFERENCE, JACCHIA VERSUS AMDB, NODRAG

Prediction interval, days	Position difference AMDB, km	Position difference NODRAG, km
0.5	11.1	6.7
1.0	44.8	27.8
5.0	1127.0	649.0

For this particular case, the nondynamic exponential model gives no better results than would be obtained from completely neglecting atmospheric drag. These results lead to the conclusion that any accurate orbit prediction program must make use of a density model that includes the three time dependent effects.

2.2.4 A new analytical atmospheric density model.- Inspection of curves in figure 3(a) suggest that, at any given time, the atmospheric density function (ordinate) may be represented by

$$-\ell n(\rho/\rho_o) = F(z) \qquad (2\text{-}2)$$

where

ρ = atmospheric density
ρ_o = reference density at sea level ($1.225\ \frac{kg}{m^3}$)
z = altitude above the oblate Earth in kilometers,

and $F(z)$ is a rational polynomial. The expression for ρ would be

$$\rho = \rho_o \exp\left[-F(z)\right] \qquad (2\text{-}3)$$

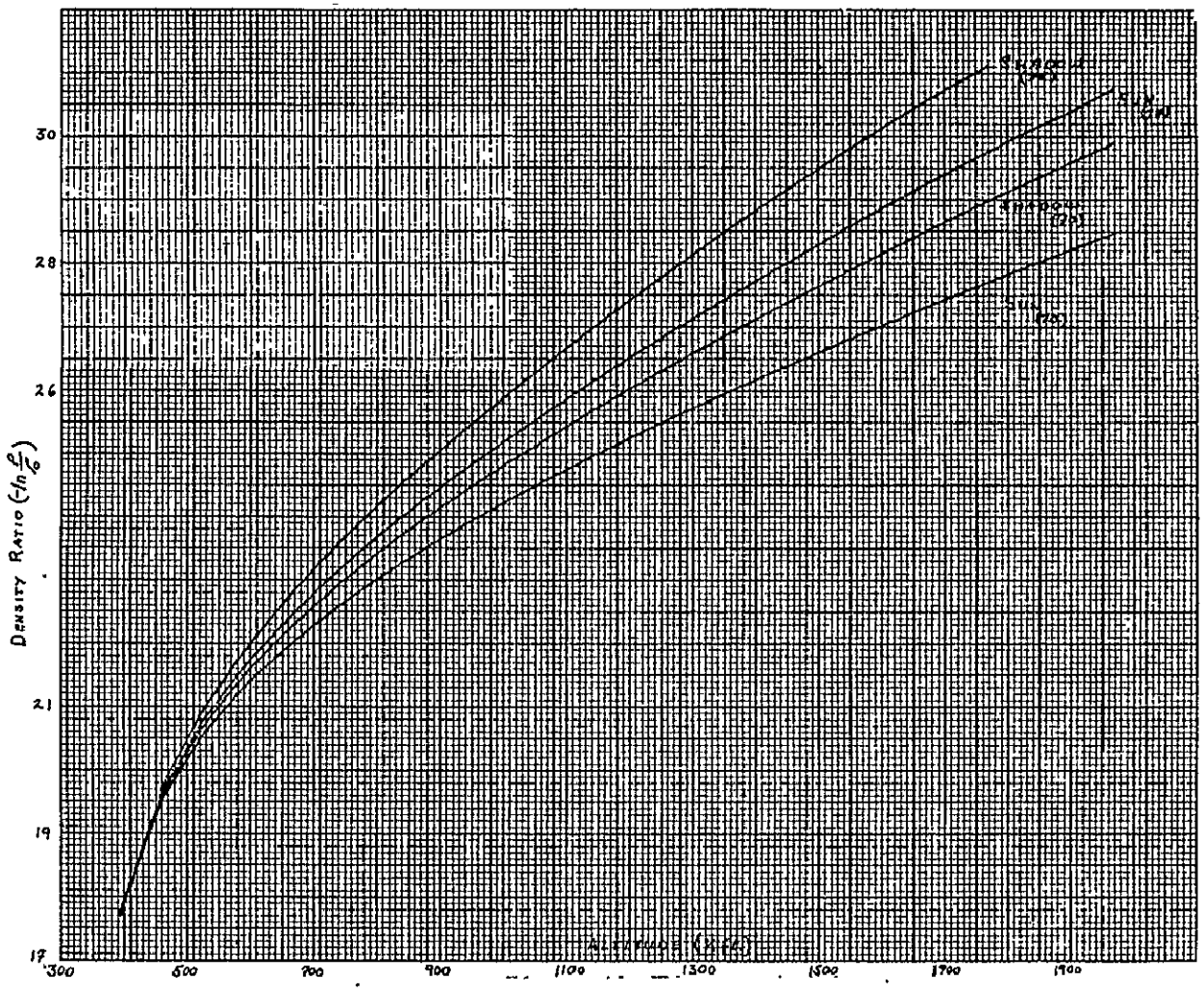

(a) Variations with altitude and epoch.

Figure 3.- Atmospheric density variations.

(b) Variations with position of the Sun at 500 km altitude.

Figure 3.- Concluded.

The coefficients in F could be determined to give agreement to the curve that corresponds to a given epoch. This procedure would account for seasonal and solar radiation intensity variations, at least over a limited time of a few days or weeks. In addition, it was thought time dependent trigonometric terms might be added to F in order to include the diurnal variations.

This approach has been used to derive a new analytical atmospheric density model (refs. 36 and 37). F in equation (2-3) is represented by

$$F = a_1 + a_2 z + \frac{a_3}{z} + B . \qquad (2-4)$$

where

$$B = -b\,(z-152)\cos(\psi-35^\circ)\cos\beta \qquad (2-5)$$

a_1, a_2, a_3 and b are constants to be determined. The function B effectively simulates the diurnal bulge of the atmosphere. ψ and β give the angular distance of the subsatellite point from the center of the bulge. Given the right ascension and declination of the Sun (α_s, δ_s) and the right ascension and declination of the vehicle (α_v, δ_v), then

$$\psi = \alpha_s - \alpha_v \qquad (2-6)$$

$$\beta = \delta_v - \delta_s \cos\psi$$

The constant of 35° in equation (2-5) represents the fact that the bulge lags 35° behind the Sun, as viewed from the surface of the Earth.

The values of a_1, a_2, a_3, are calibrated for agreement of ρ with the value predicted by the Jacchia model. Three points are chosen: $z_1 = 152$ km, $z_2 = 400$ km, $z_3 = 600$ km. They are positioned over the surface of the Earth such that $B = 0$, i.e. $\psi - 35 = \beta = \frac{\pi}{2}$. f_1, f_2, f_3 are the values of

$$-\ln\left(\frac{\rho}{\rho_o}\right)$$

as determined from the Jacchia model. Then a_1, a_2, a_3 are computed sequentially from

$$a_3 = \left[f_3 - f_1 + \frac{z_1 - z_3}{z_2 - z_1}(f_2 - f_1) \right] \Bigg/ \left[(z_1 - z_3)\left(\frac{1}{z_1 z_3} - \frac{1}{z_1 z_2} \right) \right]$$

$$a_2 = \frac{f_2 - f_1}{z_2 - z_1} + \frac{a_3}{z_1 z_2} \qquad (2\text{-}7)$$

$$a_1 = f_1 - a_2 z_1 - \frac{a_3}{z_1}$$

To compute b, choose z = 400 km and $\psi - 35^\circ = 180^\circ$, $\beta = 0$. f is obtained from the Jacchia, such that

$$b = \left(f - a_1 - a_2 z - \frac{a_3}{z} \right) \Big/ (z - 152) \qquad (2\text{-}8)$$

Equation (2-5), and hence the AMDB* model, is valid for $z \geq 152$ km. For altitudes below 152 km, the AMDB model should be used since it is in close agreement with Jacchia for that altitude range (see fig. 3(a)).

It was expected that this model would give good agreement with the Jacchia model, but require less computer storage and execution time. To investigate this concept, several orbit prediction experiments were carried out.

2.2.5 Orbit prediction experiments.- Numerical orbit predictions were carried out using the GOPP program (ref. 25). The orbits used in the comparisons are shown in table V.

TABLE V.- ORBITS USED IN PREDICTION EXPERIMENTS

	A	B	C	D	E	F
perigee (km)	220	300	300	220	Same as	166
apogee (km)	380	600	600	380	A except	433
eccentricity	.012	.022	.022	.012	epoch	.02
period (min)	90.5	93.6	93.6	90.5	is	90.5
argument of perigee	0	0	180°	0	12:00	0
ascending node	0	0	0	0	January 1,	0
inclination	30°	30°	30°	90°	1977	30°
epoch	12:00	January 1, 1975				Same as A,B,C,D

Results of the orbit prediction experiments with different density models are shown in tables VI(a) through VI(f). All comparisons are with respect to the Jacchia model. The "No Drag" case is also included.

TABLE VI.- POSITION DEPENDENCE ON DENSITY MODEL

(a) Orbit A

Time of integration, days	Position difference, km		
	No drag	RUSSIAN	AMDB*
0.5	8.9	0.2	0.3
1.0	36.1	0.8	1.5
5.0	895	16	42

(b) Orbit B

Time of integration, days	Position difference, km		
	No drag	RUSSIAN	AMDB*
0.5	.83	.03	.07
1.0	3.16	.07	.28
5.0	81.5	1.0	6.0

TABLE VI.- Continued

(c) Orbit C

Time of integration, days	Position difference, km		
	No drag	RUSSIAN	AMDB*
0.5	.5	0	.01
1.0	1.8	.02	.04
5.0	47.5	.8	.5

(d) Orbit D

Time of integration, days	Position difference, km		
	No drag	RUSSIAN	AMDB*
0.5	8.6	.1	.3
1.0	34.4	.5	1.5
5.0	836	10.3	44.9

(e) Orbit E

Time of integration, days	Position difference, km		
	No drag	RUSSIAN	AMDB*
0.5	13.9	3.4	0.4
1.0	56.0	19.2	1.9
5.0	1404	494	41.6

TABLE VI.- Concluded

(f) Orbit F

Time of integration, days	Position difference, km	
	No drag	AMDB*
0.5	40.9	.4
1.0	164.4	2.0
5.0	3944	25.9

Notes:
1. The position difference is almost entirely in the downrange direction. The largest effect of drag is to perturb the position of the satellite in its orbit.
2. All of these cases show that drag can cause a significant perturbation for orbit predictions of one day or longer.
3. The new analytical model (AMDB*) shows good agreement with Jacchia, although not quite as good as USSR for epoch in 1975.
4. For epochs other than 1975 (orbit E) the USSR model is not very accurate. This shows the effect of the solar activity level. The USSR model is based on the solar activity in 1975.
5. AMDB* has about the same accuracy, regardless of epoch. (Compare orbit A with orbit E.)

2.2.6 Additional remarks.- It has been shown that atmospheric drag can cause a large perturbation of a satellite's position in its orbit. In addition, time dependent variations in the atmospheric density can also cause large perturbations. Therefore, orbit prediction programs for near Earth orbits must include a dynamic model of the atmosphere.

The Jacchia density model has been compared with the USSR model. They show good agreement for certain orbits. The USSR model, however, is not valid for altitudes lower than 200 km or epochs other than 1975[1]. Also, both models are rather inefficient in terms of computer storage and runtime.

[1]If given the correct solar activity data, the USSR model could, perhaps, be calibrated to work for any epoch.

A new analytical model (AMDB*) has been presented. This model was developed jointly by Gus Babb (NASA/JSC), Stephen Starke (ACM) and Alan Mueller (ACM). It can be calibrated to agree with the Jacchia model at any given epoch. The chief advantages of this model are its small computer storage and execution time requirements.

Execution time[2] and storage requirements for the four models studied are shown in table VII. This data is based on the models being programed on the Univac 1110 system.

TABLE VII.- EXECUTION TIME AND STORAGE REQUIREMENTS

(Atmospheric Density Models)

Model	Execution time, ms	Storage, words
Jacchia	1.6	1252
USSR	2.6	575
AMDB	0.2	<100
AMDB*	0.3	311

It can be seen that AMDB* offers considerable advantages in speed and storage over Jacchia and USSR, and is almost as fast as the simple exponential model (AMDB). This increased speed is most useful for long orbit predictions, lifetime studies, or in applications where execution time must be limited, such as in an onboard computer.

2.3 Geopotential Model

The mathematical model for the gravitational potential of the Earth is given as a function of the satellite's position with respect to an Earth fixed coordinate system. This function is the well known solution of Laplace's equation in terms of spherical harmonics. The perturbing accelerations are obtained as the partial derivatives of the geopotential. They can be computed using nonsingular recursive equations (ref. 41).

[2]Some additional savings in execution time for the USSR could be realized if single precision programing were used.

The figure of the Earth is described by the numerical coefficients in the geopotential expansion. These coefficients have been computed from satellite observations and surface gravity measurements (ref. 42). Although they may sometimes be orbit dependent, the thorough analysis of reference 42 provides coefficients that describe the true Earth to a high precision. These coefficients were taken as the reference model for the comparisons described in this section.

Orbit predictions based on the fully determined geopotential will give the best accuracy but can be prohibitively expensive in terms of computer execution time. It is desired, therefore, to determine the effects of neglecting many of the higher order terms. Attempts were made in references 43 and 44 to determine satellite position errors resulting from predictions based on a truncated geopotential. The numerical results showed that any neglected term could produce a linear error growth. However, the analytical satellite theories and observations (table 1, ref. 42) indicate that the tesseral terms produce only periodic perturbations of small amplitude (200 nautical mile altitude). Additional numerical experiments described in this section showed that, when properly initialized, the linear error growth (due to neglected tesseral terms) in the predicted orbit could be avoided.

2.3.1 Numerical experiments.- Studies were conducted comparing a J_2 perturbed solution with a J_2 and J_{22} perturbed solution. (J_2 being the second zonal harmonic and J_{22} the second tesseral harmonic.) The J_2 perturbing potential is a function of only the position magnitude and latitude, while the J_{22} potential is a function of the position magnitude, latitude, and longitude with respect to the Earth. Two different cases were run for the J_2 versus $J_2 + J_{22}$ comparison. All were given the same inertial initial conditions. However the initial longitudes with respect to the Earth were different; i.e., different initial epochs. The initial inertial conditions were:

$a = 6677.766$ km.	$\Omega = 0.0^\circ$
$e = .015$	$\omega = 0.0^\circ$
$I = 30^\circ$	$M = 0.0^\circ$

In case 1 the hour angle was $\theta_0 = 104.8^\circ$ and in case 2, $\theta_0 = 149.9^\circ$. The position differences between the J_2 and $J_2 + J_{22}$ solutions are shown in table VIII(a) for both cases as a function of time.

As one can see from table VIII(a), case 1 appears to show a secular position difference trend stemming from the J_{22} perturbing force. While in case 2 the position difference seems to be periodic and much smaller. Case 2 verifies what has been shown analytically and from observations.

Another numerical study was made comparing an eighth order zonal model with an eighth order eighth degree zonal and tesseral model. Again two different cases for the hour angle were chosen. In case 1 the hour angle $\theta_o = 42.9$ while in case 2 $\theta_o = 100.6$. The initial conditions were the same as those in reference 44.

$a = 6629.656567$ km. $\Omega = 45^o$

$e = .01$ $\omega = 45^o$

$I = 45^o$ $M = 45^o$

The Julian date of 2442332.17 correspnds to the hour angle in case 1. The results are shown in table VIII(b).

The results in case 1, table VIII(b) are similar to those shown in reference 44. Again, table VIII(b) shows that the error growth is strongly dependent on the initial epoch.

TABLE VIII.- POSITION DEPENDENCE ON GEOPOTENTIAL MODEL

(a) 2x0 versus 2x2

Time, days	Position difference, km	
	Case 1	Case 2
0.25	1.35	0.43
.50	4.91	.005
1.0	4.07	.02
1.5	6.09	.03
2.0	19.54	.04

TABLE VIII.- Concluded

(b) 8x0 versus 8x8

Time, days	Position difference, km	
	Case 1	Case 2
.25	2.45	1.29
.50	7.3	.31
1.0	16.49	.92
1.5	24.72	1.84
2.0	28.9	2.02

2.3.2 Theoretical background.- The basic reason for the results of the two previous examples is that the right-hand side of a differential equation cannot be arbitrarily truncated without possible drastic effects on the solution. Consider the single ordinary differential equation for x,

$$\ddot{x} = F(x,t) \tag{2-9}$$

A similar differential equation for y is

$$\ddot{y} = F(y,t) + \varepsilon G(y,t) \tag{2-10}$$

where $|\varepsilon| \ll 1$ and G is periodic in y and t. Let $x^*(t)$ and $y^*(t)$ be solutions to equations (2-9) and (2-10), respectively such that

$$x^*(t_o) = y^*(t_o)$$

Define

$$\xi(t) = x(t) - y(t)$$

Then

$$\ddot{\xi} = F[\xi + y(t),t] - F[x(t) - \xi,t] - \varepsilon G[x(t) - \xi,t]$$

When ξ is initially zero,

$$\ddot{\xi} = F[\xi + y^*(t),t] - F[x^*(t) - \xi,t] - \varepsilon G[x^*(t) - \xi,t] \tag{2-11}$$

where $x^*(t)$ and $y^*(t)$ are known functions. According to the theory of differential equations, there is no reason to expect that

the solution to equation (2-11) will remain small. There is thus no theoretical justification for arbitrarily neglecting geopotential terms.

Much is known about the solutions of the differential equations in celestial mechanics. As mentioned earlier, the tesseral terms produce periodic effects in the solution. Therefore, an average over one revolution can be used to determine a "mean" mean motion that will compensate for the neglected tesseral term. The mean mean motions in case 2 (tables VIII(a) and 7(b)) agreed more closely than in case 1.

2.3.3 Comments and recommendations.- Based on the results of these studies and those documented in references 43 and 44, the following recommendations can be made:

- For very accurate predictions of satellite position (near Earth orbits) the full geopotential model must be used.
- Predictions of orbit size and shape can be based on a zonal model only.
- Mean initial elements must be used before any tesseral term can be neglected.

Practical realization of the third recommendation requires additional work in the following areas:

- Development of a rigorous theoretical justification for using initial mean elements with a simplified geopotential. This should make the connections between analytical theories and numerical solutions.
- Development of a fast numerical routine for computing initial mean values for the elements. Impact on existing programs should be minimized with the goal of minimum storage and minimum execution time for the initialization.
- Development of an efficient method for including important resonance effects. It is known that the motion of the satellite can be significantly perturbed by certain resonant geopotential terms. These cannot be neglected.

2.4 Luni-Solar Gravity Models

The gravitational forces of attraction due to the Sun and the Moon can have an important effect on the orbit of a satellite, particularly for high altitude orbits. Given the mass and position of a perturbing body, one may calculate its perturbation on the orbit.

Let $\vec{x}$ be the position vector of the satellite, referenced to some inertial coordinate system centered at the Earth. Then its acceleration is

$$\ddot{\vec{x}} + \frac{\mu}{r}\vec{x} = \vec{F}_{\leftmoon} + \vec{F}_{\odot} + \vec{R} \tag{2-12}$$

where

$$\vec{F}_{\leftmoon} = -\mu \frac{M_{\leftmoon}}{M_{\oplus}}\left(\frac{\vec{\rho}_{\leftmoon}}{\rho_{\leftmoon}^3} + \frac{\vec{r}_{\leftmoon}}{r_{\leftmoon}^3}\right)$$

$$\vec{F}_{\odot} = -\mu \frac{M_{\odot}}{M_{\oplus}}\left(\frac{\vec{\rho}_{\odot}}{\rho_{\odot}^3} + \frac{\vec{r}_{\odot}}{r_{\odot}^3}\right) \tag{2-13}$$

$$\vec{\rho}_{\leftmoon} = \vec{x} - \vec{r}_{\leftmoon}, \quad \vec{\rho}_{\odot} = \vec{x} - \vec{r}_{\odot}$$

$\vec{F}_{\leftmoon}$ and $\vec{F}_{\odot}$ are the disturbing accelerations due to the Moon and Sun, respectively, and $\vec{R}$ represents any additional accelerations. $\vec{r}_{\leftmoon}$ and $\vec{r}_{\odot}$ are the positions of the Moon and Sun, respectively, referenced to the Earth centered inertial coordinate system. The mass ratios of the Moon and Sun are known to a very high precision. The gravitational parameter is

$$\mu = k^2 M_{\oplus}$$

where k is the gravitational constant and $M_{\oplus}$ is the mass of the Earth.

The first term in the brackets of $\vec{F}_{\leftmoon}$ and $\vec{F}_{\odot}$ is called the "direct" term and represents the gravitational attraction of the satellite by the perturbing body. The second term, called the "indirect" term, represents the perturbation of the motion of the Earth. Equation (2-13) assumes point masses for the Moon and Sun. $\vec{R}$ in equation (2-12) represents perturbations such as atmospheric drag, nonsphericity of the Earth, etc.

According to equation (2-13), the luni-solar perturbing accelerations $\vec{F}_{\leftmoon}$ and $\vec{F}_{\odot}$ can be directly computed, provided that

$\vec{x}$, $\vec{r}_{\mathbb{C}}$ and $\vec{r}_{\odot}$ are known. The numerical integration of equation (2-12) requires, therefore, that the position of the Sun and Moon be known as a function of time. Two methods for obtaining this information have been investigated and are discussed in this section:

a. The stored ephemeris data on the Jet Propulsion Laboratory (JPL) tape. A polynomial interpolation is used to obtain intermediate values of $\vec{r}_{\mathbb{C}}$ and $\vec{r}_{\odot}$. This ephemeris is considered to be the most accurate available and will be used as the reference for this study. It was derived based on radar observations and satellite tracking data.

b. Analytical formulas that give the elements of the Sun and Moon as a function of time. Positions can then be computed from these elements. This type of ephemeris is sometimes preferred because it does not require the tape read and table look-up operations. However, the analytical formulas are generally not as accurate as the JPL tabulated data.

The luni-solar perturbatons will be shown for near Earth, geosynchronous and elliptical orbits. An analytical ephemeris model will be discussed and compared to the JPL model. Of particular interest are their accuracy and their computer storage and runtime requirements. Finally, suggestions are made for better utilization of a stored ephemeris.

The initial parameters of the three orbits studied are shown in table IX.

TABLE IX.- ORBITS USED IN PREDICTION EXPERIMENTS

(Luni-Solar)

	Geosynchronous, km	Near-Earth, km	Eccentric, km
h_p	35 864	220	1 000
h_a	35 864	380	39 462
e	0.0	0.012	0.723
I	0	30	30

TABLE IX.- Concluded

(Luni-Solar)

	Geosynchronous, km	Near-Earth, km	Eccentric, km
Period	24 hrs	90.5 min	12 hrs
Epoch	Noon January 1, 1975		

2.4.1 Magnitude of luni-solar perturbations.- The total effects of the Sun and Moon on the three orbits was determined by comparing the output position vectors of two cases of orbit prediction. In one case, the luni-solar gravity perturbations were included using the JPL stored ephemeris (ref. 45). Luni-solar gravity was set to zero in the other case. Results of the comparisons are shown in table X(a).

The individual effects of Sun and Moon gravity are shown in tables X(b) and X(c), respectively.

TABLE X.- LUNI-SOLAR GRAVITY EFFECTS ON POSITION

(a) Combined Sun and Moon

Prediction interval, days	Geosynchronous, km	Near-Earth, m	Eccentric, km
0.5	3.7	36.8	27.3
1	11.1	75.7	54.4
5	57.5	391.5	174.7
30	281.0	-	-

TABLE X.- Concluded

(b) Sun only

Prediction interval, days	Geosynchronous, km	Near-Earth, m	Eccentric, km
0.5	2.3	31.3	2.5
1	5.0	62.9	4.7
5	25.0	321.5	14.9
30	152.4	-	-

(c) Moon only

Prediction interval, days	Geosynchronous, km	Near-Earth, m	Eccentric, km
0.5	4.2	5.8	24.9
1	6.1	13.1	49.8
5	32.7	70.8	174.8
30	128.7	-	-

Notes:

1. The errors in each case have a linear growth. This indicates that the decision to include luni-solar perturbations in an orbit prediction depends on the expected prediction interval and required accuracy.

2. The Moon has a much larger effect than the Sun on the eccentric orbit. On the other hand, the Sun has a larger effect on the near Earth orbit.

3. Compared to air density uncertainty effects (table III), the luni-solar perturbations on a near Earth satellite are small.

4. The linear growth indicates that the source of the error is a slightly wrong value of the "mean" mean motion, similar to that discussed for the geopotential in section 2.3.

2.4.2 Analytical model versus JPL stored data.- An alternative to the JPL stored ephemeris table has been investigated in references 46 and 47. It is based on expressions that give the mean orbital elements of the Sun and Moon as functions of time, and it is therefore referred to as an analytical model.

Expressions for the Sun were obtained from the American Ephermeris and Nautical Almanac (ref. 48) and are documented in reference 46. Brown's lunar theory was used for the Moon's analytical ephemeris (source was ref. 49) and the mathematical expressions are given in reference 47. The algorithm for these analytical models will be referred to here as "ANAL." The JPL data (and associated algorithm for interpolation) will be referred to as "JPL".

The JPL AND ANAL output positions of the Sun and Moon are compared in figures 4 and 5. The differences are relatively small and periodic.

However, it must be determined how these differences affect an orbit prediction. This was done in references 46 and 47, and the results are summarized in table XI for the three types of orbits shown in table IX.

TABLE XI.- POSITION DIFFERENCE, JPL VERSUS ANAL

Prediction interval, days	Geosynchronous, km	Near-Earth, m	Eccentric, km
0.5	7	.03	22
1	5	.05	46
5	20	.4	126
30	197	-	-

Notes:
1. It is assumed that JPL is the more accurate ephemeris model since it is based on precise optical observations, spacecraft tracking and radar data.
2. The errors caused by using ANAL for orbit predictions are extremely small and are negligible for many applications.
3. The choice between JPL and ANAL must be made on the basis of operational considerations, such as execution time and storage limitations.

Computer runtime and storage comparisons are shown in table XII. While there is very little difference in execution time, JPL requires,

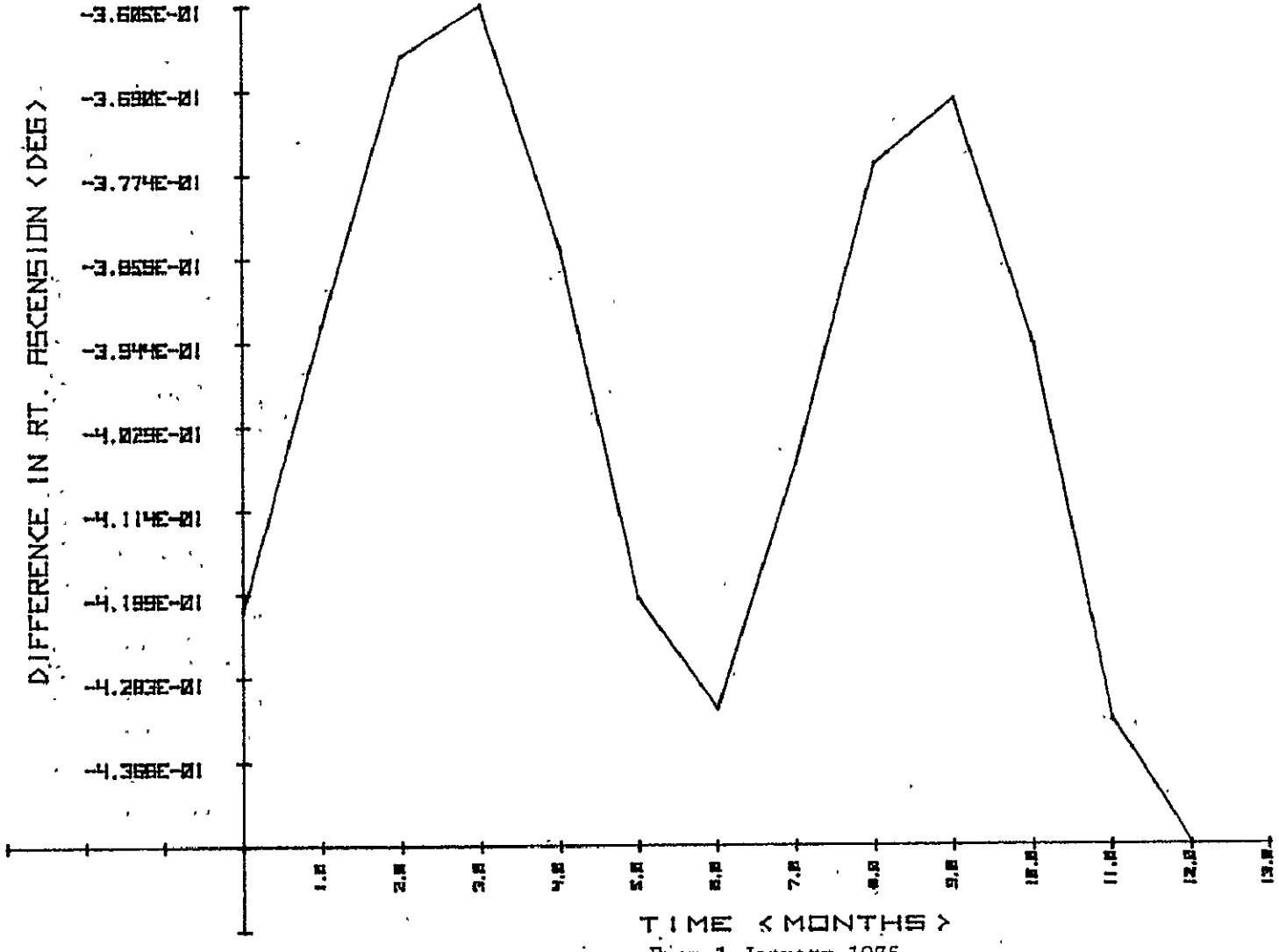

(a) Right ascension.

Figure 4.- Position of the Sun, JPL versus ANAL.

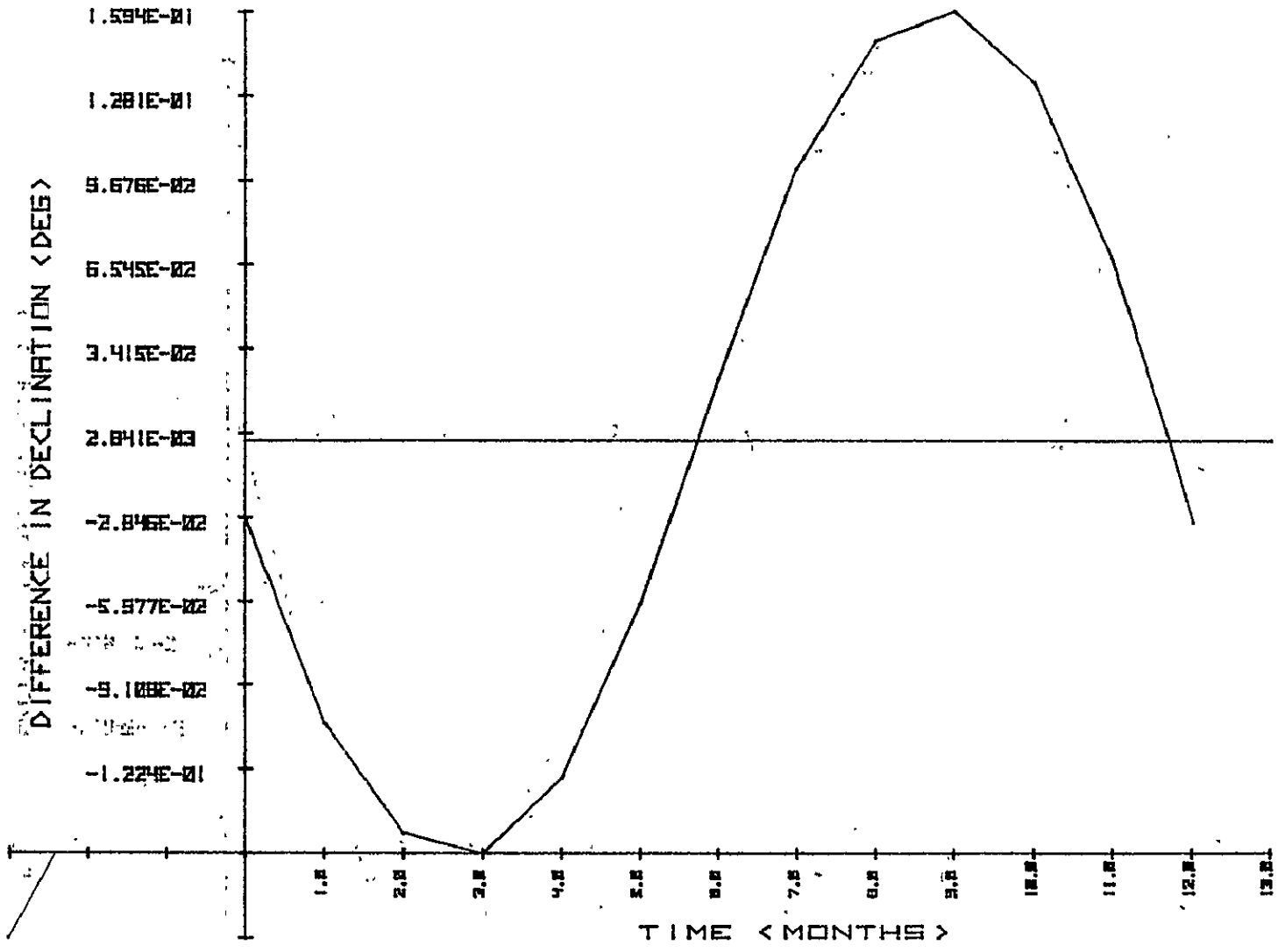

From 1 January 1975

(b) Declination.

Figure 4.- Continued.

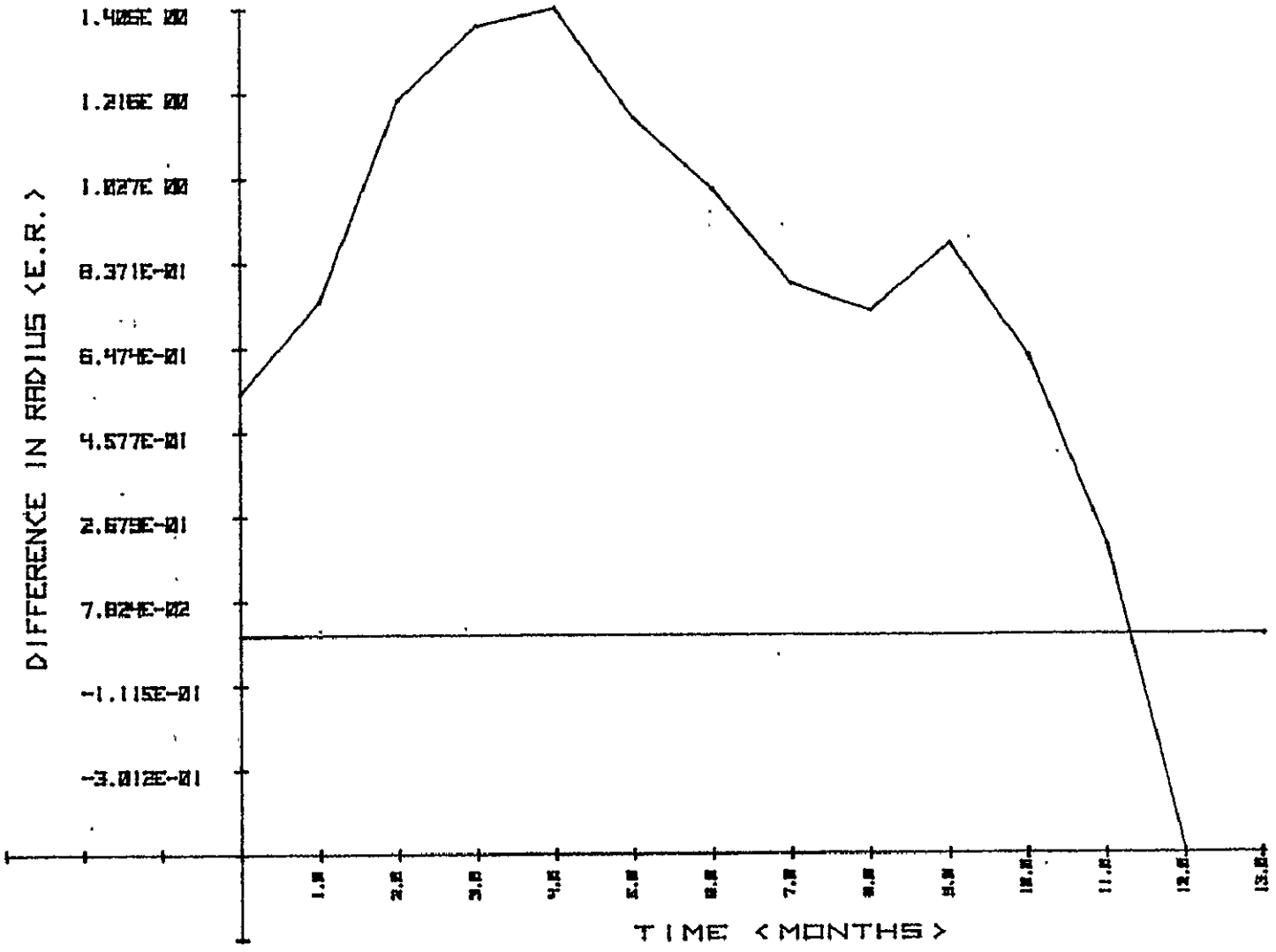

(c) Radial distance.

Figure 4.- Concluded.

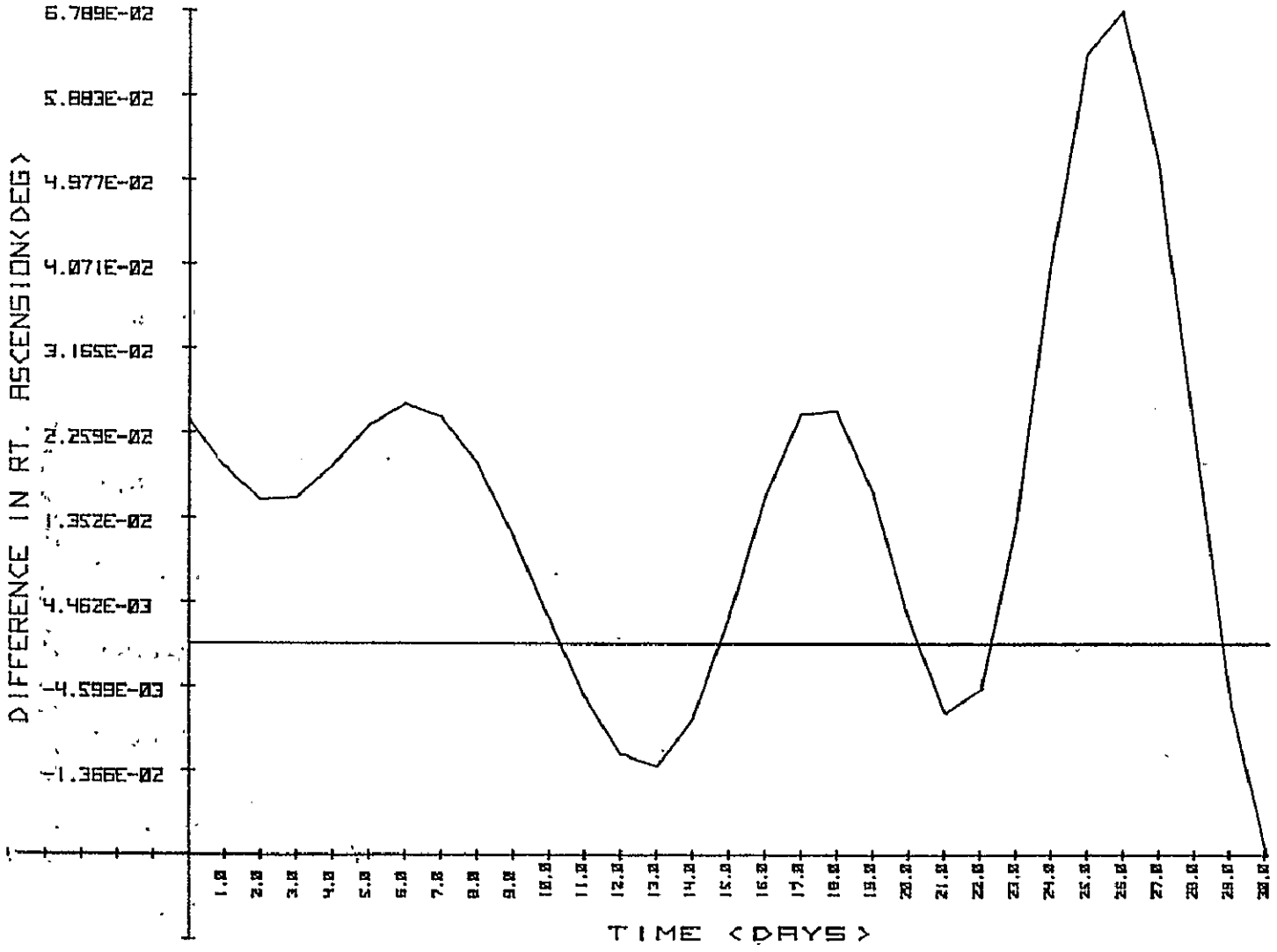

From 1 January 1975

(a) Right ascension.

Figure 5.- Position of the Moon, JPL versus ANAL.

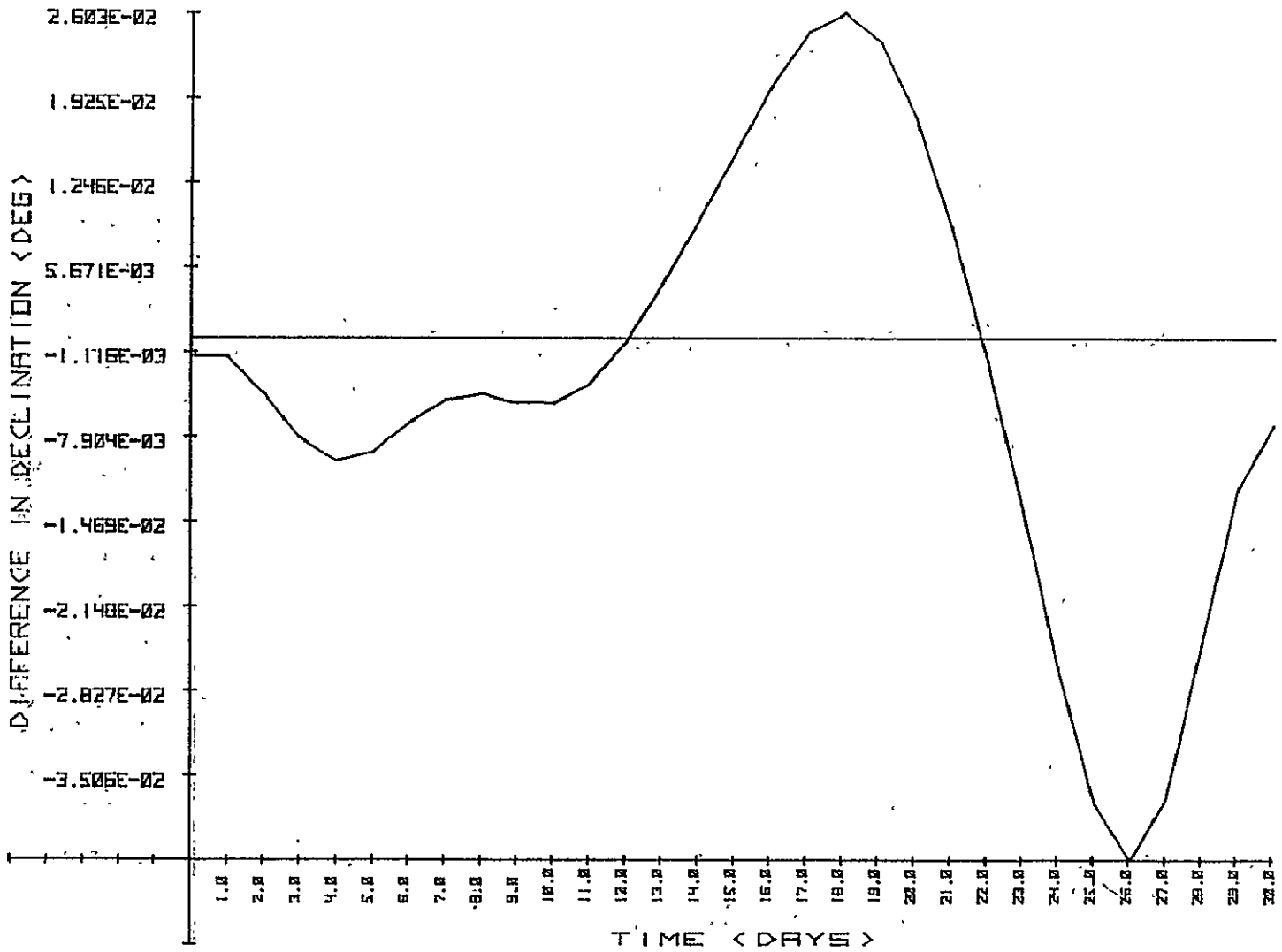

(b) Declination.

Figure 5.- Continued.

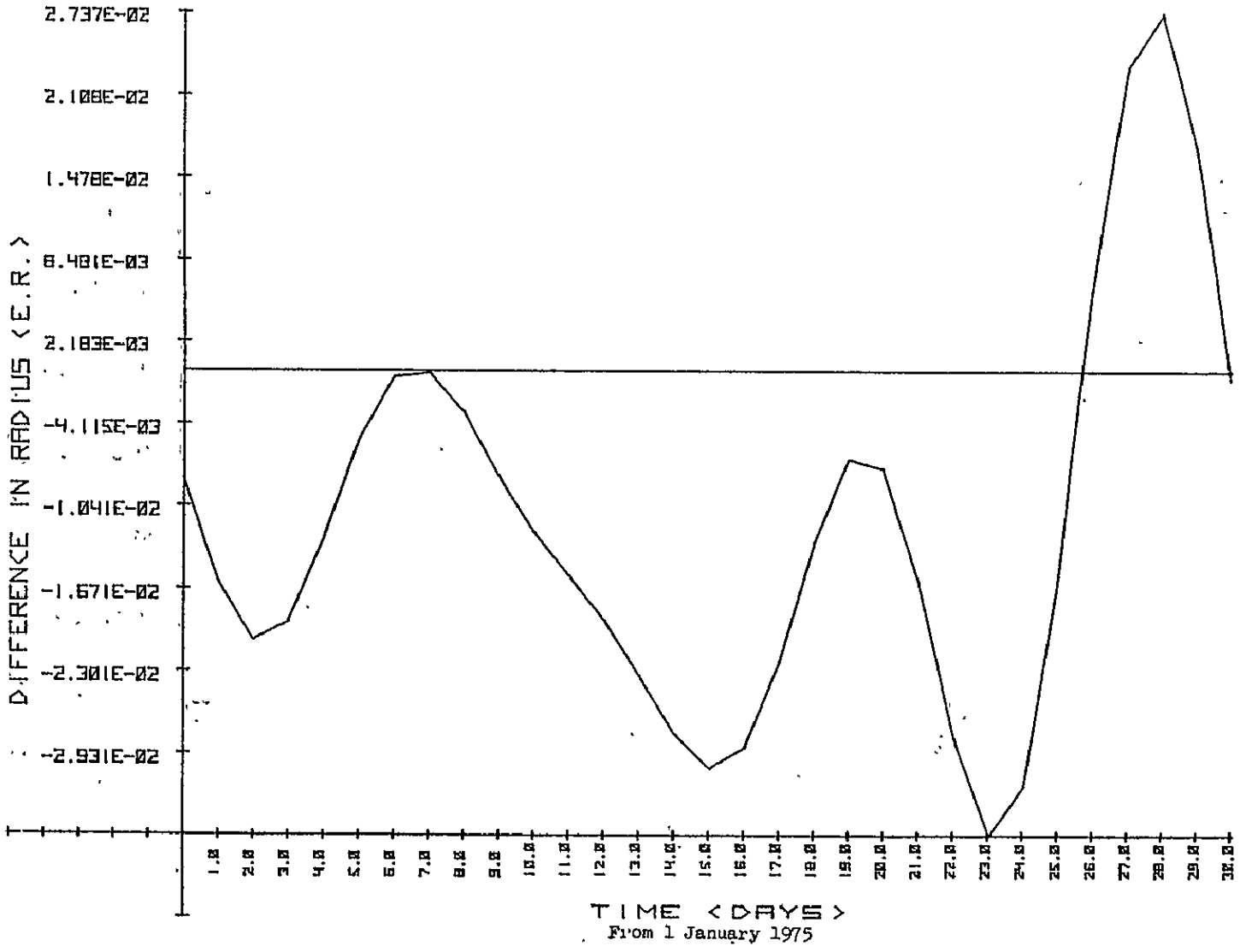

(c) Radial distance.

Figure 5.- Concluded.

on the average, 4 seconds to initialize and read the data tape. In addition, for Univac 1110 demand users, there can be a long delay while the computer operator finds and loads the magnetic tape. The demand mode also requires special procedures for the tape read during execution. Computer storage is about 50 percent more for JPL.

TABLE XII.- COMPUTER RUNTIME AND STORAGE, JPL VERSUS ANAL

Model	Execution time[a], ms	Storage, words
JPL	2.5 (4000)	1177
ANAL	2.3	766

2.4.3 Additional suggestions.- Improvements can be made to the JPL algorithm that may substantially reduce the disadvantages mentioned in the previous section. The suggested approaches are:

a. Strip the Sun and Moon data from the JPL data set. Carryout the interpolation calculations for the Sun and Moon only.

b. Place the Sun-Moon data in a more easily accessible mass storage device, such as Fastran files. This would require segmenting the data according to epoch.

c. Use Chebyschev polynomials as the interpolating functions. This would provide a bound on errors and require less data storage.

2.5 Time and Coordinate System Models

The direction in space of the Earth's rotational axis is not fixed but has two separate motions, called precession and nutation. It is usually desirable to express the geopotential accelerations in an Earth fixed coordinate system. These accelerations must then be converted to an inertial coordinate system in order to carryout the numerical integration of the satellite differential equations.

The Earth's rate of rotation is slowly decreasing. This effect, if uncorrected, can introduce errors in time. In order to correctly compute the perturbations due to the nonspherical, rotating Earth, the Earth's hour angle must be accurately known.

[a]This is the computer cost on Univac 1110 for one evaluation of the algorithm for Sun and Moon positions.

This section will discuss studies that were carried out in order to investigate the most efficient methods for including the effects of precession, nutation and Greenwich rotation in an orbit prediction program. Also to be discussed are numerical experiments that show the errors that will occur when these effects are neglected.

2.5.1 Discussion.- Precession is the steady drifting of the Earth's polar axis of rotation around the surface of a cone whose axis is the ecliptic pole and whose semicone angle is the obliquity ($23^{\circ}27'$) (see fig. 6). Period of revolution around this cone is 26 000 years, which corresponds to a drift of approximately 20 arc-seconds per anum at the Earth's pole. Suppose an inertial reference system is defined such that the Z-axis is in the direction in which the Earth's mean pole pointed on January 1, 1950. Then the Earth's pole in 1975 will differ from the Z-axis of the basic reference coordinate system by approximately 514 arc-seconds.

Define the precession matrix P to give the transformation from mean equator and equinox coordinates of some reference epoch (Basic Reference Inertial Coordinate System) to mean equator and equinox coordinates of date. The expression for this matrix is given in reference 50.

Nutation refers to the small oscillatory wobbling of the Earth's polar axis around its mean precessing position. As a result, the value of the obliquity of the ecliptic oscillates about a mean value. This transformation represents the difference between the position of the true celestial pole and the mean celestial pole. Nutation may be broken up into a series of short period terms (up to a total of 139 terms). Some of these terms have periods as small as 5 1/2 days. The two largest terms correspond to the Earth's pole traversing an ellipse of semiaxes 9".2 and 6".8 once in 18.6 years. The six largest of these terms were included in the study.

Thus, the nutation matrix N makes the transformation from mean equator and equinox coordinates of date to true equator and equinox coordinates of date. Explicit expressions for the matrix N as a function time are given in reference 50.

Greenwich rotation is the daily rotation of the Earth around its own spin axis. The rate of rotation of the Earth was derived by Newcomb in 1895. His equation became the definition of "non-uniform" time commonly called universal time, UT1. The amount of rotation of the Earth is given in terms of UT1 rather than the angle called the Greenwich mean sideral time. In the analysis, Greenwich mean sideral time is obtained from UT1. The explicit expression for the Greenwich rotation (matrix G) is given in reference 50.

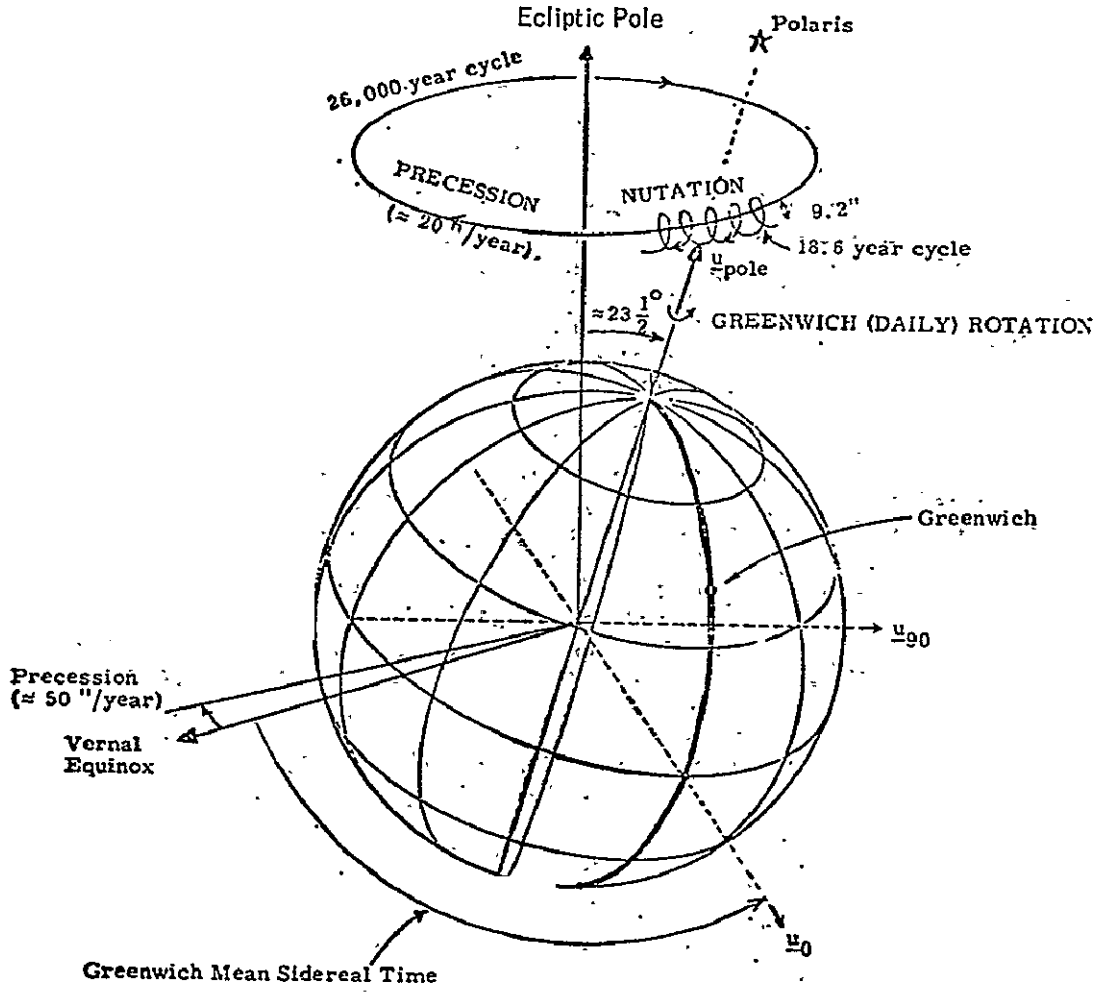

Figure 6.- Precession nutation, and Greenwich rotation.

To summarize this discussion, the entire transformation from basic reference inertial coordinates to Earth-fixed coordinates, and vice versa, can be given by the matrix product GNP as follows:

$$r_{EF} = G\ N\ P\ r_{IC}$$

or

$$r_{IC} = P^T N^T G^T\ r_{EF}$$

where r_{IC} and r_{EF} are vectors in the reference coordinates and Earth-fixed coordinates, respectively.

2.5.2 Numerical experiments.- The expressions for matrices G, N, and P are lengthy, containing many trigonometric functions. It is, therefore, desirable when numerically predicting satellite orbits to minimize the number of times these matrices need to be calculated. A study was carried out to determine the effect of precession, nutation and nonuniform Greenwich rotation on a near Earth satellite orbit and to determine the optimum way to implement these effects in orbit prediction programs.

Two methods of approach were taken. In one, the matrices G, N, and P are computed at each function evaluation (calculation of perturbing forces). This method will be referred to here as GNP. In the second method of approach, these matrices were computed once at the epoch of initialization and held constant (till epoch time is changed, if ever). This method will be referred to here as GNP*. GNP and GNP* were compared with neglecting totally the effects due to precession, nutation and nonuniform Greenwich rotation (referred to as GNP**).

In GNP**, the transformation from basic reference to Earth-fixed system and vice versa is accomplished by

$$r_{EF} = R_{uniform} \left[G\ N\ P\right]_{Epoch} r_{IC}$$

$$r_{IC} = \left[G\ N\ P\right]^T_{Epoch} R^T_{uniform}\ r_{EF}$$

where $R_{uniform}$ is a rotation matrix giving a uniform rotation of the Earth.

$$R_{uniform} = \begin{bmatrix} \cos\ \omega_E t & \sin\ \omega_E t & 0 \\ -\sin\ \omega_E t & \cos\ \omega_E t & 0 \\ 0 & 0 & 0 \end{bmatrix}$$

ω_E is the rate of uniform rotation of the Earth at initialization epoch, and $[G\ N\ P]_{Epoch}$ is the exact transformation matrix from basic reference to Earth-fixed system at initialization epoch. Thus ω_E and $Q = G\ N\ P$ are computed once and $R_{uniform}$ is computed at each function evaluation.

The example considered has the following initial conditions:

Height of perigee	200 km
Height of apogee	400 km
Eccentricity	0.015
Period	90.0 min
Inclination	30 deg
Epoch	Noon, January 1, 1975
Perturbations	Full 18x18 geopotential No drag No luni-solar forces

Input, output, and integration are in inertial coordinates. The results are displayed in tables XIII(a), XIII(b) and XIV. All numerical integrations were done in the mean of 1950 basic reference coordinate system.

TABLE XIII.- TIME AND COORDINATE SYSTEM COMPARISONS

(a) GNP versus GNP*

Prediction interval, days	Error in position, km	GNP CPu time, sec
1.0	negligible	163
2.0	0.00025	328
10.0	0.0121	1640
30.0	0.0540	4926

Notes:
1. For this case, the coordinate systems and time of GNP and GNP* coincide at the initialization of the orbit prediction.
2. In order to compute the perturbing accelerations of the nonspherical Earth, the satellite's postion vector

is rotated into an Earth-fixed coordinate system, using GNP or GNP*.

3. GNP* is fixed (except for the uniform rotation of Greenwich) whereas GNP is changing slowly. The small deviation between the two, results in the errors in position shown above.

4. The errors in position result from the effects of precession, nutation and time errors over 1, 2, 10 and 30 days.

5. These errors remain small, growing to be only 50 meters at 30 days. For predictions of several months, the GNP* matrix should probably be updated every 3 or 4 months.

(b) GNP* versus GNP**

Prediction interval, days	Error in position, km	GNP CPu time, sec
0.0623	1.0	8
0.25	5.7	30
0.75	6.2	88
1.0	9.2	117
2.0	11.9	233

Notes: 1. The GNP* matrix is computed in the same manner as for table XIII(a). However, GNP** contains only the uniform Greenwich rotation from the mean of 1950 coordinate system.

2. Again, the satellite position vector is rotated from the inertial to an Earth-fixed coordinate system, using GNP* or GNP**.

3. The position errors shown above result from the accumulated precession and nutation from 1950 to 1975 (the epoch of the orbit prediction). For GNP**, the Earth has the wrong orientation with respect to the inertial coordinate system. The perturbing accelerations will

therefore be in error. The integral of these acceleration errors results in the accumulated errors shown above.

4. The large errors indicate that an orbit prediction program must account for precession, nutation and nonuniform rotation of the Earth.

TABLE XIV.- EXECUTION TIME COMPARISONS (GNP)

GNP	GNP*	GNP**
48%	2%	0.0

Notes: 1. Computer cpu execution times are compared here. Since GNP** requires the least calculations, its execution time is taken as the reference for percentage comparisons.

2. The total execution times for GNP and GNP* are shown in table XIII(a) and XIII(b), respectively.

3. The GNP case requires a 48% increase in execution time whereas GNP* requires negligible additional time.

2.5.3 Conclusions.- Based on these results, it is concluded that the precession, nutation and nonuniform time equations can be evaluated once at initialization of the orbit prediction and held constant thereafter. This is the method of implementation in the GOPP and KSFAST programs (refs. 25 and 28). An error of about 50 meters will accumulate (for a nearly circular, near Earth orbit) after 30 days. Therefore, for predictions over an extended time period, GNP* should be updated every 3 or 4 months.

2.6 Recommendations Based on Orbit Types

It is the purpose of this section to make recommendations on the appropriate force models to be used for orbit prediction based on the type of orbit under consideration. These recommendations are based on the models analyzed in the previous sections. Certain additional force models (such as solar radiation pressure and vehicle venting) may be needed for some satellites.

It is difficult to make general recommendations because of the large diversity of satellite missions and objectives. The

following recommendations are directed primarily to the shuttle orbiter missions and the transfer and geosynchronous orbits of its payload.

The orbit types to be considered here are: near Earth orbits with small eccentricities, elliptical transfer orbits, and geosynchronous orbits. The size and shape of each is given by the semimajor axis a and eccentricity e. The prediction interval to be considered is T.

2.6.1 Near-Earth orbits.-

Orbital characteristics: $6500 \text{ km} < a < 7200 \text{ km}$
$0 < e < 0.05$
$0 < T < 2$ days

Force model recommendations for this class of orbits:

a. Geopotential - all the terms of a chosen model (such as ref. 42) should be used; i.e., all the terms that were used in the reduction of satellite observation data[1].

b. Atmospheric density - the dynamic model AMDB* should be used. A small increase in accuracy may be realized with the Jacchia model (computer cost will also be increased, however).

c. Luni-solar gravity - these amount to about 80 meters in downrange position (after 1 day) and can usually be neglected. This depends, however, on the prediction interval since this error increases linearly. At 5 days, the error is 400 meters.

d. Precession, nutation, nonuniform rotation - the GNP* method should be used.

2.6.2 Near-Earth orbit lifetime studies.-

Orbital characteristics: $6550 \text{ km} < a < 7200 \text{ km}$
$0 < e < 0.05$
several months $< T <$ several years

---

[1]The order and degree of models can vary. It is important to realize, however, that each coefficient of a given model may have nearly equal weight for a near Earth satellite. As an example, $C_{18,17}$ may be as physically important as $C_{8,7}$ since all coefficients (S_{ij}, C_{ij}, $i=2,3,\cdots,N$, $j=0,1,\cdots,i$) are computed as a set.

Force model recommendations for this class of orbits:

a. Geopotential - same as section 2.6.1

b. Atmospheric density - same as section 2.6.1

c. Luni-solar gravity - Sun and Moon gravity effects should be included, using the analytical ephemeris model.

d. Precession, nutation, nonuniform rotation - the GNP* method should be used, with update intervals of a few months.

2.6.3 Elliptical transfer orbits.-

Orbital characterisitcs: $20\,000 \text{ km} < a < 25\,000 \text{ km}$
$.65 < e < .75$
$0 < T < 5$ days

Force model recommendations for this class of orbits:

a. Geopotential - since the orbit passes near the Earth, the complete model should be used. However, near apogee the higher terms will be insignificant and can be neglected. An automatic procedure for doing this has been implemented in the program KSFAST (see ref. 28).

b. Atmospheric density - the AMDB* or Jacchia model should be used, but only when the altitude is less than about 700 km. Above that altitude, the drag calculation should be automatically skipped.

c. Luni-solar gravity - the high altitude at apogee requires that Sun and Moon gravity be included. The analytical model of section 2.4 is recommended (error is .06 km after 5 days).

d. Precession, nutation, nonuniform rotation - the GNP* method should be used.

2.6.4 Geosynchronous orbits.-

Orbital characteristics: $a \tilde{=} 42240$ km

$e \tilde{=} 0.0$
$0 < T < 30$ days

Force model recommendations for this class of orbits:

a. Geopotential model - The major contribution of the high order geopotential terms is long period resonant motion. Therefore, a fourth order and fourth degree model is recommended. For predictions of longer than 30 days, additional tesseral terms may be needed. In any case, terms of higher order than 16 will be lost in

the roundoff errors of Univac 1110 double precision arithmetic, and should not be included.

b. Atmospheric density - atmospheric drag can be neglected for this case.

c. Luni-solar gravity - the analytical ephemeris model may be used, provided that errors on the order of 0.2 km (after 30 days) are acceptable.

d. Precession, nutation, nonuniform rotation - The GNP* model can be used.

2.6.5 General results.- The discussion in section 2.6 concerns the recommended models of atmospheric density, nonspherical Earth, luni-solar gravitation, coordinate systems and nonuniform Greenwich rotation. These force models and the three orbit types do not, admittedly, cover all the existing and proposed satellite missions. However, the results can be a useful help in designing an orbit prediction program. In the event that additional orbit types and force models need to be considered, a short analysis based on the procedures used here could produce a more accurate program requiring less computer runtime. Results contained in this report are an excellent starting point for such an analysis.

Listed below are the important general results of these studies that apply to all orbit prediction problems.

- Periodic variations in atmospheric density need to be included when air drag is important. These variations can cause a 100 percent change in the effects of air drag on the orbit.
- Numerical calculation of atmospheric density can be carried out with single precision (Univac 1110) arithmetic. In addition, the solar ephemeris in a dynamic model (such as Jacchia and AMDB*) can be obtained from a "mean" Sun on a circular orbit. The result is a 50 percent decrease in the computer cost of the density model evaluation, and no loss of accuracy.
- The geopotential model (except for the J_2 term) can also be evaluated in single precision without loss of accuracy. The geocoefficients (table 18, ref. 42) are given to 5 decimal digits. Therefore, intermediate calculations in single precision (7 to 8 decimal digits, Univac 1110) are sufficiently accurate[1].

[1]This assumes that there are no "programing errors" such as taking the sum of a large number and a small number or the difference of two large, nearly equal numbers.

- The calculation of the precession and nutation matrices as well as the expression for nonuniform Greenwich rotation needs to be done only at the initialization of the orbit prediction. For very long predictions (several months or more) the values may need to be updated, depending on the accuracy requirements of the prediction.

- For orbits passing near the Earth (200-400 km) it is necessary to include all the known terms in the geopotential model. The reason is that, near the Earth, all the term (except J_2) have about the same magnitude.

  Neglecting any term results in an error in the "mean" mean motion that accumulates linearly in the downrange direction.

- For prediction intervals of a few days, the luni-solar gravitational effects on a near Earth orbit (200-400 km) can, in many cases, be neglected. This results in typical downrange positron errors of 0.4 km after 5 days. With the shuttle orbiter, for example, these errors are much less than those resulting from uncertainites in aerodynamic drag.

REFERENCES

1. Roy, A.: The Foundations of Astrodynamics. Macmillan Co., 1965.

2. Janin, G.: Accurate Computation of Highly Eccentric Satellite Orbits. Celestial Mechanics, vol. 10, Dec. 1974.

3. Pines, S.: Variation of Parameters for Elliptical and Near Circular Orbits. Astronomical Journal, vol. 66, no. 1, 1961, p. 1286.

4. Pines, S.: Averaged Initial Cartesian Coordinates for Long Lifetime Satellite Studies. Flight Mechanics/Estimation Theory Symposium, X-582-75-273, Aug. 1975.

5. Dallas, S. S.; and Rinderle, E. A.: A Comparison of Cowell's Method and a Variation-of-Parameters Method for the Computation of Precision Satellite Orbits. Journal of Astronautical Sciences, vol. XXI, no. 3 and 4, 1974.

6. Burdet, C. A.: Theory of Kepler Motion: The General Perturbed Two-body Problem. Zeitchrift fuer Angewandte Mathetic and Physik, vol. 19, 1968.

7. Silver, M.: A Short Derivation of the Sperling-Burdet Equations of Motion for Perturbed Two-Body Problem. Celestial Mechanics, vol. 11, Feb. 1975.

8. Stiefel, E.; and Scheifele, G.: Linear and Regular Celestial Mechanics. Springer-Verlag, 1971.

9. Bond, V. R.; and Hanssen, V.: The Burdet Formulation of the Perturbed Two-Body Problem with Total Energy as an Element. JSC IN 73-FM-86, 1973.

10. Bond, V. R.: The Development of the Poincare-Similar Elements with Eccentric Anomaly as the Independent Variable. JSC IN 75-FM-16, Mar. 1975.

11. Scheifele, G.; and Graf, O.: Analytical Satellite Theories Based on a New Set of Canonical Elements. AIAA Paper 74-838, 1974.

12. Bond, V.; and Scheifele, G.: An Analytical Singularity-Free Solution to the J_2 Perturbation Problem. JSC IN (to be published).

13. Graf, O. F.: A Discussion and Comparison of Numerical Integration Methods for Computing Satellite Orbits. JSC IN 76-FM-47, July 1975.

14. Baumgarte, J.; and Stiefel, E.: Stabilization by Manipulation of the Hamiltonian. Celestial Mechanics, vol. 10, pp. 77-85, 1974.

15. Henrici, P.: Discrete Variable Methods in Ordinarly Differential Equations. John Wiley and Sons (New York), 1962.

16. Lapidus, L.; and Seinfeld, J.: Numerical Solution of Ordinary Differential Equations. Academic Press, 1971.

17. Fehlberg, E.: Low-Order Classical Runge-Kutta Formulas with Stepsize Control and Their Application to Some Heat Transfer Problems. NASA TR R-315, 1969.

18. Fehlberg, E.: Classical Fifth-, Sixth-, Seventh-, and Eighth-Order Runge-Kutta Formulas with Stepsize Control. NASA TR R-287, 1968.

19. Fehlberg, E.: Some Experimental Results Concerning the Error Propagation in Runge-Kutta Type Integration Formulas. NASA TR R-352, 1970.

20. McAdoo, S. E.: Comparison of Coefficients for Low Order Runge-Kutta Integrators. JSC Memorandum FM53 (75-23), June 24, 1975.

21. Shanks, E.: Solutions of Differential Equations by Evaluations of Functions. Mathematics of Computation, Vol: 20, 1966.

22. Moore, H.: Comparison of Numerical Integration Techniques for Orbital Applications. Proceedings for the Conference on Numerical Solution of Ordinary Differential Equations, 1972. Springer-Verlag (Berlin), 1974.

23. Mueller, A.: Comparison of Two Types of Total Energy Elements. JSC IN 76-FM-94, Dec. 1976.

24. Bond, V. R.: Numerical Integration of Hamiltonian Systems of Differential Equations. JSC IN 75-FM-71, Oct. 1975.

25. Ouseph, E.: User's Guide and Software Documentation for the General Orbit Propagation Program (GOPP). JSC IN 75-FM-30, June 1975.

26. Wang, P.: User's Guide and Theoretical Background for ANALYT: An Analytical Orbit Propagation program. JSC IN 75-FM-62, Sept. 9, 1975.

27. Ouseph, E.: A Comparison of the Analytical Orbit Propagator (ANALYT) and the Numerical Orbit Propagator (KSFAST). ACM Memo 120, Jan. 7, 1976.

28. Mueller, A.; and Ouseph, E.: A Satellite Orbit Prediction Program (KSFAST). JSC IN 76-FM-42, July 30, 1976.

29. Graf, O.: An Error Estimate for Multirevolution Integration Methods. AIAA Paper 84-840, Aug. 1974.

30. Graf, O.: Multirevolution Methods for Orbit Integration. Proceedings for the Conference on Numerical Solutions of Ordinary Differential Equations, Austin, Texas, 1972. Lecture notes in Mathematics, vol. 362, p. 471, Springer-Verlag, Heidelberg.

31. Graf, O.: Documentation and User's Guide for the Multirevolution Orbit Prediction Program (KSMULT). JSC IN 76-FM-44, Aug. 30, 1976.

32. Ouseph, E.: Comparison of the Orbit Prediction Programs KSMULT and KSFAST for Near Earth Orbits. ACM Memo 142, Sept. 10, 1976.

33 Ouseph, E.: A General Multirevolution Orbit Prediction Program (STEPR). JSC IN 76-FM-103, Dec. 1976.

34 Graf, O.: Atmospheric Density Model Effects on the Computation of Satellite Trajectories. ACM Memo 121, Jan. 14, 1976.

35 Starke, S.: Diurnal Effects of the Sun on the Upper Atmospheric Density. ACM Memo 123, Feb. 2, 1976.

36 Starke, S.: A New Analytical Atmospheric Density Model. ACM Memo 128, Apr. 14, 1976.

37 Mueller, A.: An Improved Atmospheric Density Model. ACM Memo 140, Sept. 3, 1976.

38 Babb, G.; and Bean, W.: Analytical Atmospheric Density Model. JSC Memorandum FM5 (75-4), 1975.

39 Jacchia, L.: New Static Models of the Thermosphere and Exosphere with Empirical Temperature Profiles. Smithsonian Astrophysical Observatory Special Report.

40 Elyasberg, P.; et al.: Upper Atmosphere Density Determination from the Cosmos Satellite Deceleration Results. Space Research XII, p. 727, Akademic-Verlag, Berlin, 1973.

41. Mueller, A. C.: A Fast Recursive Algorithm for Calculating the Forces Due to the Geopotential. JSC IN 75-FM-42, June 1975.

42. Gasposchkin, E. M.: 1973 Smithsonian Standard Earth (III), Special Report 353, Smithsonian Astrophysical Observatory, Nov. 28, 1973.

43. Mueller, A. C.: Some Preliminary Results of Force Model Study for Near Earth Orbits. ACM Memo 112, July 1975.

44. Kirkpatrick, J. C.: The Theory of the Potential Applied to Orbit Prediction. JSC IN 76-FM-9, Feb. 1976.

45. Henry, E.: A Double Precision Fortran Computer Program (GPFEM) for a General Purpose Lunar and Planetary Ephemeris. MSC IN 67-FM-8, 1967.

46. Starke, S.: Comparison of Numerical Integration of Earth Satellite Orbits by Using an Analytical Ephemeris Model as Opposed to Ephemeris Data from the JPL Tape for the Sun and the Moon. ACM Memo 131, June 1, 1976.

47. Mueller, A.: Comparison of Brown Lunar Ephemeris to the JPL-Tape Read Ephemeris. ACM Memo 136, June 21, 1976.

48. Explanatory Supplement to the Astronomical Ephemeris and the American Ephemeris and Nautical Almanac. London, Her Majesty's Stationery Office, 1961.

49. Battin, R.: Astronautical Guidance. McGraw-Hill, 1964, pp. 379-383.

50. Ouseph, E.: Implementation of Precession, Nutation and Non-Uniform Rotation of the Earth in GOPP and KSFAST. ACM Memo 122, Jan. 23, 1976.

DISTRIBUTION FOR JSC IN 77-FM19

JM2/Center Data Management (3)
JM6/Tech. Library (2)
FA/Dir. of Data Systems and Analysis
FA/Tech. Asst. for Space Shuttle
FE/C. H. Woodling
FE3/C. C. Olasky
FR/Chief
FS/Chief
FM/R. L. Berry
FM/E. L. Davis
FM/R. H. Brown
FM2/Chief
FM2/K. A. Young
M. D. Jenness
R. W. Becker
FM6/Chief
E. M. Fridge
G. Weisskopf
R. S. Davis
D. M. Braley
FM4/Chief
J. D. Yencharis
J. C. Harpold
A. J. Bordano
FM8/Chief
W. R. Wollenhaupt
FM15/Chief
V. R. Bond (5)
FM14/Report Control Files (25)
FM/Author (5)
LA/Manager
LM/Manager
SAMSO/XRZ/D. R. Collins
P. O. Box 92960
Los Angeles, CA 90009
IBM/59/W. Bridges (2)
MDAC/W. Hayes (2)
IBM/L. Burnett
IBM/B. Goodyear
AT/J. Loftus
NASA Hdq/M. Savage
L. Roberts
W. Miller
Dr. P. Kurtzhals
GSFC/C. L. Maskaleris/512
L. Anderson/572